



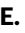




# Repurposed drugs and their combinations prevent morbidity-inducing dermonecrosis caused by diverse cytotoxic snake venoms

Received: 24 May 2022

Accepted: 11 November 2023

Published online: 14 December 2023

 Check for updates

Steven R. Hall <sup>1,2</sup>, Sean A. Rasmussen <sup>3</sup>, Edouard Crittenden<sup>1</sup>, Charlotte A. Dawson <sup>1</sup>, Keirah E. Bartlett <sup>1</sup>, Adam P. Westhorpe<sup>1</sup>, Laura-Oana Albulescu<sup>1,2</sup>, Jeroen Kool <sup>4,5</sup>, José María Gutiérrez <sup>6</sup> & Nicholas R. Casewell <sup>1,2</sup> ✉

Morbidity from snakebite envenoming affects approximately 400,000 people annually. Tissue damage at the bite-site often leaves victims with catastrophic life-long injuries and is largely untreatable by current antivenoms. Repurposed small molecule drugs that inhibit specific snake venom toxins show considerable promise for tackling this neglected tropical disease. Using human skin cell assays as an initial model for snakebite-induced dermonecrosis, we show that the drugs 2,3-dimercapto-1-propanesulfonic acid (DMPS), marimastat, and varespladib, alone or in combination, inhibit the cytotoxicity of a broad range of medically important snake venoms. Thereafter, using pre-clinical mouse models of dermonecrosis, we demonstrate that the dual therapeutic combinations of DMPS or marimastat with varespladib significantly inhibit the dermonecrotic activity of geographically distinct and medically important snake venoms, even when the drug combinations are delivered one hour after envenoming. These findings strongly support the future translation of repurposed drug combinations as broad-spectrum therapeutics for preventing morbidity caused by snakebite.

Current estimates suggest that 1.8–2.7 million people are envenomed due to snakebite every year, resulting in 81,000–138,000 deaths and 400,000 cases of morbidity annually, predominantly affecting those in the tropics and sub-tropics<sup>1–3</sup>. One of the leading causes of snakebite-induced morbidity is local tissue necrosis, which can develop around the bite site and result in amputation of the affected digit or limb in survivors<sup>1,4</sup>. Snakebite has been labelled ‘the most neglected of neglected tropical diseases (NTDs)’<sup>5</sup>, with the late UN Secretary General Kofi Annan calling it ‘the biggest public health crisis you have likely never heard of’<sup>6</sup>. In 2017, snakebite envenoming was

added to the World Health Organization (WHO)’s formal list of NTDs; the WHO has since elevated snakebite to a ‘priority category A NTD’ and has created a roadmap with the goal of reducing the global burden of snakebite by one-half by the year 2030<sup>7</sup>. One of the proposed methods to accomplish this is to develop novel treatments for snakebite; an ambitious task considering the myriad issues associated with developing snakebite therapies, including the variability and complexity of toxins that make up different snake venoms<sup>8,9</sup>.

Snake venoms are comprised of dozens of different toxins at varying concentrations, which differ both inter- and intra-specifically

<sup>1</sup>Centre for Snakebite Research & Interventions, Liverpool School of Tropical Medicine, Pembroke Place, Liverpool L3 5QA, UK. <sup>2</sup>Centre for Drugs & Diagnostics, Liverpool School of Tropical Medicine, Pembroke Place, Liverpool L3 5QA, UK. <sup>3</sup>Department of Pathology and Laboratory Medicine, Queen Elizabeth II Health Sciences Centre and Dalhousie University, 7th Floor of MacKenzie Building, 5788 University Avenue, Halifax, NS B3H 1V8, Canada. <sup>4</sup>Division of BioAnalytical Chemistry, Amsterdam Institute of Molecular and Life Sciences (AIMMS), Vrije Universiteit Amsterdam, De Boelelaan 1085, 1081 HV Amsterdam, The Netherlands. <sup>5</sup>Centre for Analytical Sciences Amsterdam (CASA), 1098 XH Amsterdam, The Netherlands. <sup>6</sup>Instituto Clodomiro Picado, Facultad de Microbiología, Universidad de Costa Rica, PO Box 11501-2060 San José, Costa Rica. ✉ e-mail: [nicholas.casewell@lstmed.ac.uk](mailto:nicholas.casewell@lstmed.ac.uk)

and induce a range of pathological and pathophysiological effects<sup>8</sup>. However, there are four primary toxin families that are dominant across many different venoms and thus represent attractive targets for toxin-inhibiting therapeutics: phospholipases A<sub>2</sub> (PLA<sub>2</sub>s), snake venom metalloproteinases (SVMs), snake venom serine proteases (SVSPs), and three-finger toxins (3FTxs)<sup>10</sup>. The main syndromes of snakebite envenoming are generally categorised as haemotoxic (e.g. haemorrhage and coagulopathy), neurotoxic (e.g. muscle paralysis), and/or cytotoxic (e.g. local tissue necrosis)<sup>11,12</sup>. Haemotoxicity is a particularly common sign of envenoming, especially following bites from viperid (family Viperidae) snakes, and is largely caused by SVMs, SVSPs, and PLA<sub>2</sub>s<sup>11–13</sup>. Neurotoxic envenoming is more commonly caused by elapid (family Elapidae) snakes and is primarily associated with neurotoxic 3FTxs and PLA<sub>2</sub>s<sup>12,14</sup>. Local tissue necrosis around the site of the bite is caused by both vipers and certain elapids, is the result of cytotoxic 3FTxs, SVMs, and PLA<sub>2</sub>s, and frequently leads to permanent disability often requiring surgical debridement or amputations of the affected limb or digit<sup>15,16</sup>.

The only treatments currently available for snakebite envenoming are animal-derived polyclonal antibody therapies called antivenoms. These therapies have conceptually remained unchanged for over a century and are associated with a multitude of issues including high cost, requirement for a consistent cold-chain, limited cross-snake species efficacy due to venom variation, and high frequency of adverse events post-administration<sup>1,8,9,17–20</sup>. In addition, they need to be administered intravenously (IV) in a clinical environment by a medical professional, which severely restricts their utility in rural communities where snakebite victims are often hours or even days away from appropriate facilities<sup>1,9,21</sup>. Finally, due to the large size of antivenom antibodies or their fragments (i.e. typically ~50 kDa, Fab; ~110 kDa, F(ab')<sub>2</sub>; or ~150 kDa, IgG) these treatments are unable to efficiently penetrate into peripheral tissue surrounding a bite-site thus reducing their efficacy against local tissue cytotoxicity, resulting in several studies determining that antivenoms are largely ineffective clinically at preventing local tissue necrosis, despite their apparent life-saving properties against the systemic effects of snakebite envenoming<sup>1,22–26</sup>. To address some of these considerable challenges, next-generation snakebite therapies, such as toxin-specific monoclonal antibodies<sup>27,28</sup> and toxin-inhibiting small molecule drugs<sup>29–35</sup>, have received considerable attention in recent years.

Small molecule drugs offer many desirable characteristics in comparison to existing conventional antivenoms, such as potential increased cross-species efficacy, tolerability, stability, and affordability<sup>9,32,33,35</sup>. However, due to the irreversibility and rapid development of venom-induced local tissue necrosis any potential novel snakebite therapy will have to be quickly administered to effectively prevent such pathology<sup>25,36</sup>. Because of their small size, drugs are amenable to be formulated as oral, topical or locally injectable (i.e. subcutaneous or intradermal) therapies which could be administered in the field much more quickly after a bite compared to an IV-administered antivenom<sup>9,31,32,35,37–39</sup>, thus providing considerable theoretical potential to reduce the permanent sequelae associated with cytotoxic snake venoms<sup>36</sup>. Of particular interest is the development of intradermal (ID) delivery microinjection devices containing venom toxin-inhibiting drugs, which could be self-administered by victims themselves directly to the site of the bite immediately after the event<sup>40,41</sup>.

Three repurposed drugs initially developed for other conditions<sup>32,42,43</sup> have shown particular promise as potential drug therapies for snakebite envenoming based on in vitro and in vivo data: the SVM-inhibiting metal chelator, DMPS (Unithiol)<sup>32</sup>, the hydroxamic acid, marimastat<sup>33,34,36,44,45</sup>, and the secretory PLA<sub>2</sub>-inhibiting drug, varespladib<sup>29,34,46–49</sup>. Additionally, it has been shown that combining marimastat with varespladib improves their pan-geographic utility, resulting in superior prevention of venom-

induced lethality in mice compared with either drug alone against diverse snake venoms<sup>33</sup>. While these studies have demonstrated such drugs can effectively protect against snake venom-induced lethality in animal models, there is limited published evidence of their efficacy or potential utility against local tissue necrosis.

Herein we explore the therapeutic potential of small molecule drugs against the local tissue damage stimulated by cytotoxic snakebite envenoming. Using a variety of geographically diverse snake venoms we demonstrate that DMPS, marimastat, and varespladib individually provide protection against snake venom cytotoxins to different extents, but that drug combinations are highly effective at preventing local tissue damage in vivo, even when delivered up to 60 minutes after venom challenge, and thus represent promising leads for combatting the local dermonecrotic effects caused by snakebite envenoming.

## Results

### Diverse snake venoms inhibit human epidermal keratinocyte viability

Prior to exploring the inhibitory capability of drugs against the cytotoxic effects of snake venoms, we defined the effect of 11 venoms sourced from distinct snake species and geographic regions on the viability of adherent human skin cells. Using 3-(4,5-dimethylthiazol-2-yl)-2,5-diphenyl tetrazolium bromide (MTT) assays<sup>50,51</sup> and immortalised human epidermal keratinocytes (HaCaT<sup>52,53</sup>), we generated venom dose-response curves (Fig. 1a–k). MTT assays measure two types of venom action on adherent cells: direct inhibition of cell viability<sup>50,51</sup> and cellular detachment from the culture plate (an effect that can be caused by certain SVMs, such as BAH1<sup>54</sup>), both of which evidence the deleterious actions of venoms on the keratinocytes. Using a broad concentration range for each venom and measuring the resulting viability of adherent cells after 24 hours, we calculated the concentration at which cell viability was inhibited for each venom by 50% (IC<sub>50</sub> values; Fig. 1l) as a measure of potency. Our results demonstrated that 9 of the 11 venoms tested displayed similar potencies, with those from the vipers *Bitis arietans* (puff adder, sub-Saharan Africa), *Bothrops asper* (fer-de-lance, Central America), *Crotalus atrox* (Western diamondback rattlesnake, North America), *Calloselasma rhodostoma* (Malayan pit viper, South East Asia), *Echis carinatus* (Indian saw-scaled viper, South Asia and the Middle East) and *Echis ocellatus* (West African carpet viper, West Africa) (IC<sub>50</sub> range: 7.5–19.6 µg/mL) comparable to those from the elapid spitting cobras *Naja nigricollis* (black necked spitting cobra, West Africa and East Africa variants) and *Naja pallida* (red spitting cobra, East Africa) (IC<sub>50</sub> range: 23.1–27.2 µg/mL). The venom of *Daboia russelii* (Russell's viper, South Asia; IC<sub>50</sub>: 45.1 µg/mL) was slightly, albeit significantly, less potent than that of the other vipers *B. asper*, *C. atrox*, *C. rhodostoma*, *E. carinatus*, and *E. ocellatus*, while venom from the primarily neurotoxic non-spitting cobra, *Naja haje* (Egyptian cobra) (IC<sub>50</sub>: 86.8 µg/mL), was the least potent with a significantly higher IC<sub>50</sub> value than all other tested venoms. None of the resulting Hill slopes, measures of the steepness of each venom's dose-response curve, were significantly different from each other, though all 11 were greater than |−1| (Fig. 1m), suggesting likely 'positive cooperativity' between venom toxins<sup>55,56</sup>.

### DMPS and marimastat reduce the loss of adherent cell viability stimulated by certain snake venoms

Prior to investigating the inhibitory potency of toxin-inhibiting drugs in the MTT assay, we determined the cellular 'maximum tolerated concentration (MTC)' of the repurposed drugs DMPS, marimastat, and varespladib. Thus, HaCaT cells were treated with two-fold serial dilutions of each drug until a significant reduction in cell viability was observed after 24 hours of exposure. The highest concentration of each drug that did not significantly reduce cell viability when compared to the vehicle control (labelled '0') was determined to be the

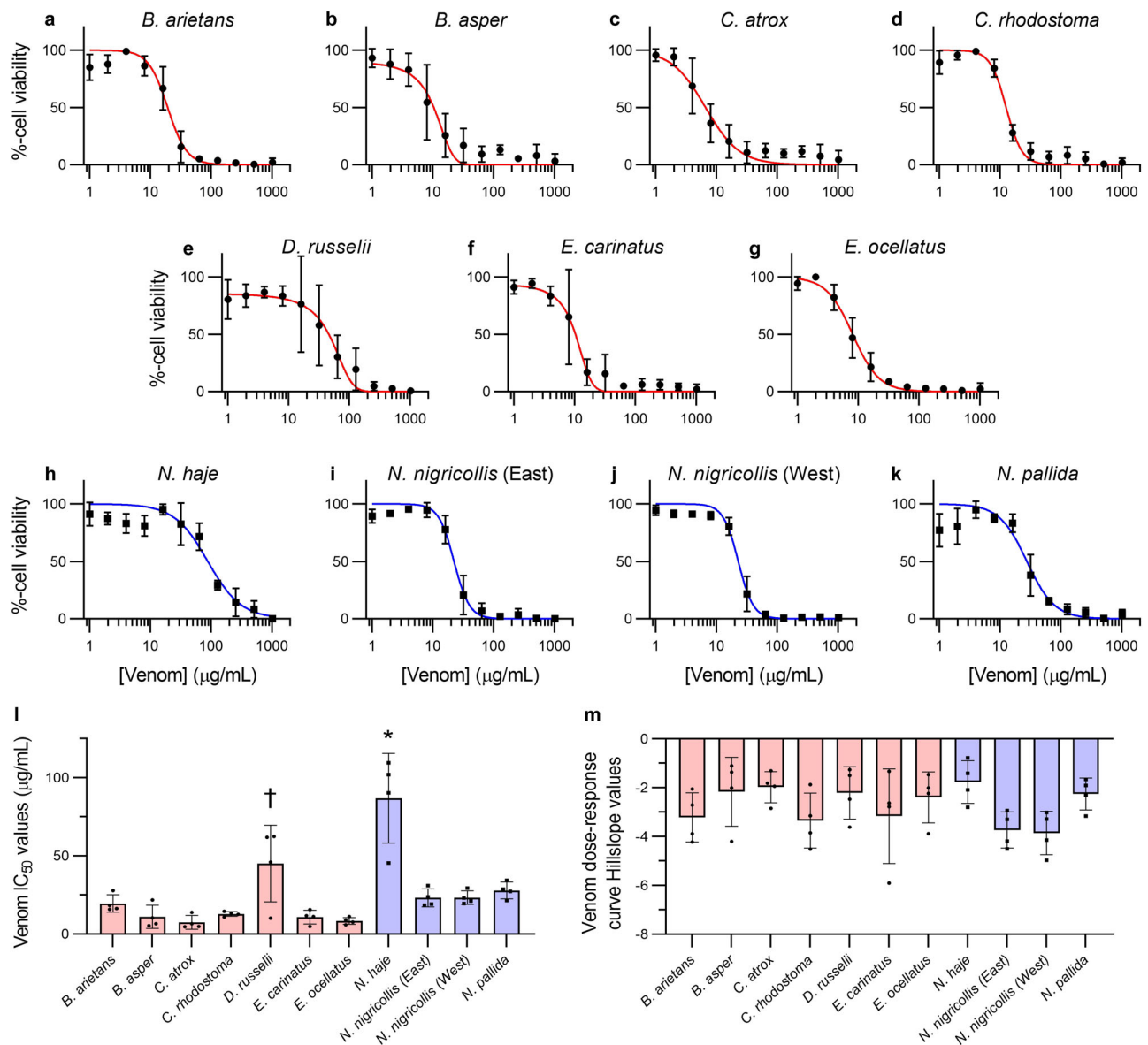


**Fig. 1 | Snake venoms dose-dependently inhibit HaCaT adherent cell viability.** MTT cell viability assays were completed in adherent HaCaT epidermal keratinocytes exposed to serial dilutions (1–1,024 μg/mL) of different snake venoms for 24 hours. The venoms tested were from **a** *Bitis arietans*, **b** *Bothrops asper*, **c** *Crotalus atrox*, **d** *Colloselasma rhodostoma*, **e** *Daboia russelii*, **f** *Echis carinatus*, **g** *Echis ocellatus*, **h** *Naja haje*, **i** East African *Naja nigricollis*, **j** West African *Naja nigricollis*, and **k** *Naja pallida*. **l** IC<sub>50</sub> and **m** Hill slope values were calculated for each independent trial. Red-coloured data denotes viperid snakes, while blue-coloured data denotes elapid snakes. \* Signifies that the value is significantly higher than all other

tested venoms, and † signifies that the value is significantly higher than *B. asper*, *C. atrox*, *C. rhodostoma*, *E. carinatus*, and *E. ocellatus*, as determined by a one-way ANOVA comparing all values to each other followed by a Tukey's multiple comparisons test ( $P < 0.05$ ,  $n = 4$  biologically independent cell experiments). ANOVA statistics for individual statistically analysed graphs are: **l**  $F(10,33) = 14.47$ ,  $P = 0.0000000022$ ; **m**  $F(10,33) = 1.828$ ,  $P = 0.0942$ . Data are presented as mean values  $\pm$  SD and the individual IC<sub>50</sub> and Hill slope values for each trial are shown as points within the bars of the graphs in **l** and **m**. Source data are provided as a Source Data file.

MTC. Then, to ensure that cells would be treated with a sub-toxic amount of drug in the venom-inhibition experiments, one half of this dose (MTC<sub>1/2</sub>) was selected for the venom-drug co-treatment experiments<sup>57,58</sup>. The MTC<sub>1/2</sub> for DMPS, marimastat, and varespladib used in the following experiments were 625, 2.56, and 128 μM, respectively (Supplementary Fig. 1).

Next, using a drug pre-incubation model<sup>32,33</sup> followed by MTT assays in the HaCaT cells, we tested the inhibitory effect of the three toxin-inhibiting drugs (using their MTC<sub>1/2</sub> values) against six of our previously tested cytotoxic snake venoms. Our results demonstrated that the SVMP inhibitors DMPS and marimastat<sup>32,33,44</sup> significantly ( $P < 0.05$ ) reduced the cell-damaging potency of venom from *C. atrox*, *E. carinatus*, and *E. ocellatus* (Fig. 2b–d, respectively), as demonstrated

by the increased IC<sub>50</sub> values. Additionally, DMPS slightly, albeit significantly, increased the IC<sub>50</sub> of East African *N. nigricollis* venom ( $P = 0.0053$ ) (Fig. 2e), though its effect was not significant against West African *N. nigricollis* venom ( $P = 0.0501$ ) (Fig. 2f). In contrast, the PLA<sub>2</sub>-inhibitor varespladib<sup>29</sup> did not display an inhibitory effect on any of the six tested venoms. The cell viability-inhibitory effects of *B. arietans* and West-African *N. nigricollis* (Fig. 2a–f) venom were not significantly inhibited by any of the tested drugs.

**DMPS and marimastat, but not varespladib, inhibit PLA<sub>2</sub>-rich *D. russelii* and *B. asper* venom-induced cytotoxicity in cell culture** Due to the surprising lack of inhibitory effect observed with varespladib in the MTT cell viability studies summarised in Fig. 2, we

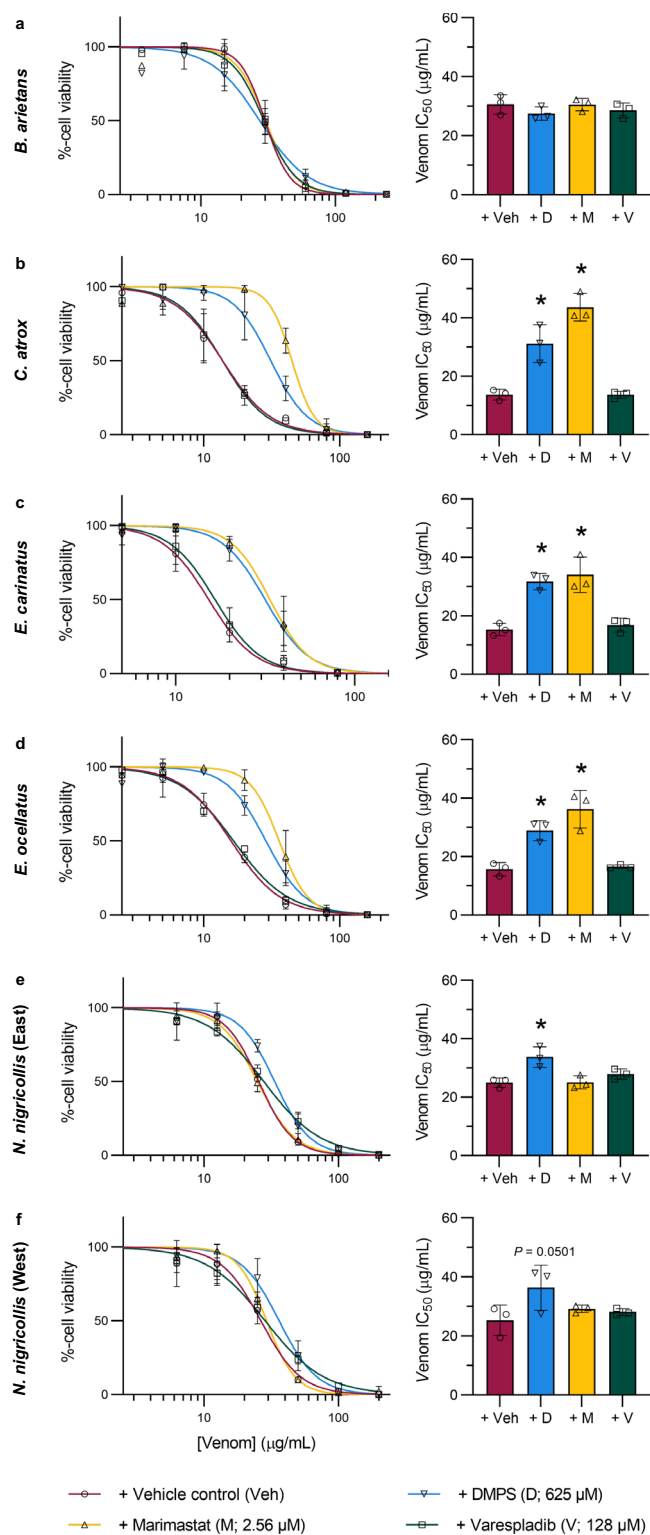


**Fig. 2 | DMPS and marimastat, but not varespladib, inhibit the potency of certain cytotoxic snake venoms in adherent HaCaT cells.** Serial dilutions of venoms (2.5–200 µg/mL) were pre-incubated with the MTC<sub>1/2</sub> of DMPS, marimastat, varespladib, or vehicle control for 30 minutes, after which HaCaT cells were exposed to the treatments for 24 hours followed by MTT cell viability assays, from which venom concentration-response curves and their associated IC<sub>50</sub> values were calculated. Panels show venom from **a** *B. arietans*, **b** *C. atrox*, **c** *E. carinatus*, **d** *E. ocellatus*, **e** East African *N. nigricollis*, and **f** West African *N. nigricollis*. \* Signifies that the IC<sub>50</sub> is significantly higher than that of the vehicle control for that venom as determined by a one-way ANOVA followed by Dunnett's multiple comparisons test ( $P < 0.05$ ,  $n = 3$  biologically independent cell experiments). ANOVA statistics for individual statistically analysed graphs are: **a**  $F(3,8) = 1.057$ ,  $P = 0.4195$ ; **b**  $F(3,8) = 37.16$ ,  $P = 0.000048$ ; **c**  $F(3,8) = 21.17$ ,  $P = 0.0004$ ; **d**  $F(3,8) = 20.34$ ,  $P = 0.0004$ ; **e**  $F(3,8) = 8.757$ ,  $P = 0.0066$ ; **f**  $F(3,8) = 2.998$ ,  $P = 0.0952$ . Data are presented as mean values  $\pm$  SD and the individual values for each trial are shown as points within each of the bar graphs. Source data are provided as a Source Data file.

measured by either MTT or PI assays against either of these viper venoms (Fig. 3). None of the drugs significantly inhibited *D. russelii* venom potency as measured with MTTs, though DMPS reduced its potency as measured with PI (Fig. 3a, b). Both DMPS and marimastat inhibited *B. asper* venom potency as measured by MTT, while only marimastat did so as measured by PI (Fig. 3c, d).

#### Varespladib potentiates the inhibitory activity of marimastat against *B. asper* venom in cells when used in combination

Although the findings described in Figs. 2 and 3 suggest that the cytotoxic activity of the viper venoms under study is primarily mediated by SVMP toxins, we wanted to determine whether PLA<sub>2</sub> inhibition by varespladib could potentiate the cytoprotective properties of the SVMP-inhibiting drugs DMPS and marimastat in a representative venom abundant in PLA<sub>2</sub> toxins. Thus, we repeated the MTT and PI assays using *B. asper* venom and compared the protective effects of combination treatments with those conferred by individual drug therapies. While no drug-potential effect was observed when varespladib was combined with DMPS (Fig. 4a, b), when combined with marimastat such potentiation was apparent as the potency of *B. asper* venom was significantly reduced compared to the marimastat-alone treatment, as measured with both MTT and PI assays (Fig. 4c, d).

#### Toxin-inhibiting drugs species-specifically reduce the formation of venom-induced dermal lesions in vivo, while drug combinations provide broad pan-species efficacy

An in vivo experimental animal model was used to assess the preclinical efficacy of the three toxin-inhibitory drugs and the corresponding rationally selected drug combinations at preventing the formation of venom-induced dermal lesions. We first used this model (based on the minimum necrotic dose [MND] model<sup>61</sup>) to determine appropriate intradermal (ID) doses of *B. asper* and *C. atrox* venom that elicit the formation of sufficiently large dermal lesions without causing any evident systemic envenoming effects, which we found to be 150 and 100 µg, respectively (Supplementary Fig. 2). A 39 µg dose of *E. ocellatus* venom was previously determined<sup>62</sup>. Next, we co-incubated the venom doses or PBS vehicle control with drug vehicle control (98.48% PBS, 1.52% DMSO), DMPS (110 µg), marimastat (60 µg), varespladib (19 µg), DMPS & varespladib (110 and 19 µg, respectively), or marimastat & varespladib (60 and 19 µg, respectively) for 30 minutes at 37 °C, prior to ID-injecting the venom-plus-drug treatments into separate groups of five mice each. To allow sufficient time for dermonecrosis to fully develop the mice were euthanised after 72 hours<sup>61</sup> (unless otherwise indicated), after which their skin lesions were excised, photographed, and measured. Representative images and the full image set of the resulting lesions are shown in Fig. 5a and Supplementary Fig. 3, respectively. No lesions were observed in the drug-only controls (Fig. 5b). *B. asper* venom caused a mean lesion area of 41.9 mm<sup>2</sup> which,

decided to repeat these experiments using venoms from *D. russelii* and *B. asper*, which have higher PLA<sub>2</sub> toxin abundances proportionally than the other six tested venoms<sup>10</sup>, and to increase the concentration of varespladib from its MTC<sub>1/2</sub> (128 µM) to its MTC (256 µM). In addition, propidium iodide (PI) cell death assays<sup>59,60</sup> were multiplexed with the MTT assays as secondary measures of the cytotoxic potencies of the venoms, in case varespladib was incompatible with the MTT assays. Despite the potential for more abundant PLA<sub>2</sub> toxins to contribute to cell cytotoxic effects, varespladib again showed no inhibition as

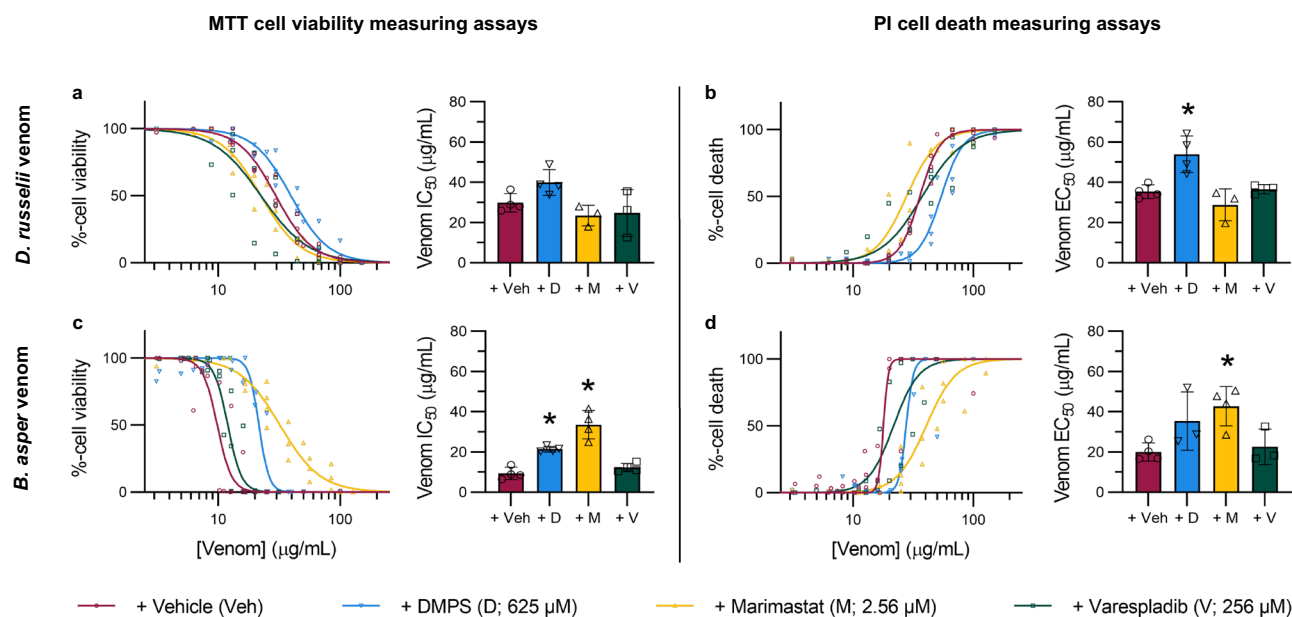


**Fig. 3 | SVMP inhibitors reduce the loss of HaCaT cell viability and/or cell death stimulated by *D. russelii* and *B. asper* venoms.** HaCaT cells were treated for 24 hours with serial dilutions of *D. russelii* (3.125–100 µg/mL, top row) or *B. asper* (2.2–127 µg/mL, bottom row) venom that had been pre-incubated with drug vehicle control, DMPS (625 µM), marimastat (2.56 µM), or varespladib (256 µM). For all treatment groups, MTT cell viability (LHS of figure) and PI cell death (RHS of figure) assays were performed. \* Signifies that value is significantly different than that of the vehicle control for that venom as determined by a one-way ANOVA followed by

Dunnett's multiple comparisons test ( $P < 0.05$ ,  $n = 3$  [a{M,V}, b{M, V}, d{D, V}] or 4 [a{Veh, D}, b{Veh, D}, c{Veh, D, M, V}, d{Veh, M}] biologically independent cell experiments). ANOVA statistics for individual statistically analysed graphs are: **a**  $F(3,10) = 3.969$ ,  $P = 0.0422$ ; **b**  $F(3,10) = 10.14$ ,  $P = 0.0022$ ; **c**  $F(3,12) = 29.20$ ,  $P = 0.0000085$ ; **d**  $F(3,10) = 4.677$ ,  $P = 0.0273$ . Data are presented as mean values  $\pm$  SD and the individual values for each trial are shown as points within each of the graphs. Source data are provided as a Source Data file.

in contrast to the cell data, was not significantly reduced by marimastat (55.1 mm<sup>2</sup>) but was by varespladib (12.2 mm<sup>2</sup>). Although DMPS (21.1 mm<sup>2</sup>) visually appeared to reduce the mean lesion area caused by *B. asper* venom, this was not statistically significant ( $P = 0.1535$ ) (Fig. 5c). *C. atrox* venom caused a mean lesion area of 19.1 mm<sup>2</sup>, which was significantly reduced in size by all three drug treatments: DMPS (3.1 mm<sup>2</sup>), marimastat (4.4 mm<sup>2</sup>) and, again in contrast to the cell data, varespladib (5.8 mm<sup>2</sup>) (Fig. 5d). *E. ocellatus* venom caused a mean lesion area of 5.0 mm<sup>2</sup>. In contrast with the other two venoms, varespladib was ineffective at reducing the lesion size (7.0 mm<sup>2</sup>). Both SVMP inhibitors appeared to substantially reduce *E. ocellatus* venom-induced lesions, with all five marimastat-treated and four of the five DMPS-treated mice displaying no lesions; however, only the effects observed with marimastat were significant (0 mm<sup>2</sup>), while those of DMPS were not due to the single outlier value in this treatment group (1.0 mm<sup>2</sup>,  $P = 0.0856$ ) (Fig. 5e).

Using the same in vivo methods, we then tested combination therapies consisting of the PLA<sub>2</sub>-inhibiting varespladib with the SVMP-inhibiting DMPS or marimastat against these same three venoms. In contrast to the single drug therapies, which displayed variable efficacies depending on the snake species and rarely completely inhibited lesion formation in individual mice, both combination therapies significantly inhibited lesion formation caused by all three venoms tested, with many individual mice displaying no lesion development at all (Fig. 5, Supplementary Fig. 3). Thus, mean *B. asper* venom-induced lesions (41.9 mm<sup>2</sup>) were decreased to 2.7 and 6.7 mm<sup>2</sup> (Fig. 5c), *C. atrox* lesions (19.1 mm<sup>2</sup>) to 0.3 and 0.3 mm<sup>2</sup> (Fig. 5d), and *E. ocellatus* lesions (5.0 mm<sup>2</sup>) to 0.1 and 0.4 mm<sup>2</sup> (Fig. 5e) by the DMPS and varespladib and marimastat and varespladib combination therapies, respectively.

### Histopathological analysis of lesions confirms SVMP- and PLA<sub>2</sub>-inhibiting drugs and their combinations protect against snake venom-induced dermonecrosis

To better understand the dermal pathology induced by the snake venoms in vivo with and without co-incubation with DMPS,

marimastat, varespladib, or their combinations, cross sections of the lesions shown in Fig. 5 were prepared, formalin-fixed, paraffin-embedded and stained with haematoxylin & eosin (H&E) dye. Photomicrographs were taken of each section at 100X magnification (10X objective, 10X ocular) for analysis and a severity scoring system was developed, which expanded upon the recent work of Ho et al.<sup>63</sup>. The severity of dermonecrosis within each skin layer (epidermis, dermis, hypodermis, panniculus carnosus, and adventitia) was scored between 0 and 4 by two blinded experimenters, with 0 representing 0% of the layer within the image being affected, 1 representing up to 25%, 2 representing between 25–50%, 3 representing between 50–75%, and 4 being the most severe and representing >75% of the skin layer (Supplementary Fig. 4). An overall dermonecrosis score was then calculated from the mean of the resulting scores obtained for the various layers (Fig. 6). Representative photomicrographs of no, partial, and heavy dermonecrosis are shown in Fig. 6a–c.

The drug treatments plus venom vehicle control induced no dermonecrosis (Fig. 6d, Supplementary Fig. 4a). Varespladib and the combination therapies consisting of DMPS or marimastat with varespladib decreased *B. asper* venom-induced dermonecrosis in the epidermis, dermis, hypodermis, and panniculus carnosus layers, though not in the adventitia, while neither DMPS nor marimastat alone inhibited the effects of *B. asper* venom in any of the skin layers (Supplementary Fig. 4b). This collectively resulted in varespladib and the two combination treatments decreasing the overall mean dermonecrosis score induced by *B. asper* venom from 2.57 to 0.72, 0.06, and 0.32, respectively, while DMPS and marimastat were ineffective (Fig. 6e). All treatments decreased *C. atrox* venom-induced dermonecrosis in the epidermis and dermis, and all but varespladib did so in the hypodermis, though no treatment had a significant effect in the panniculus carnosus or adventitia (Supplementary Fig. 4c). This resulted in the various treatments decreasing the overall mean dermonecrosis score induced by *C. atrox* venom from 2.86 to 0.04–1.32 (Fig. 6f). Lastly, marimastat and the two combination therapies significantly

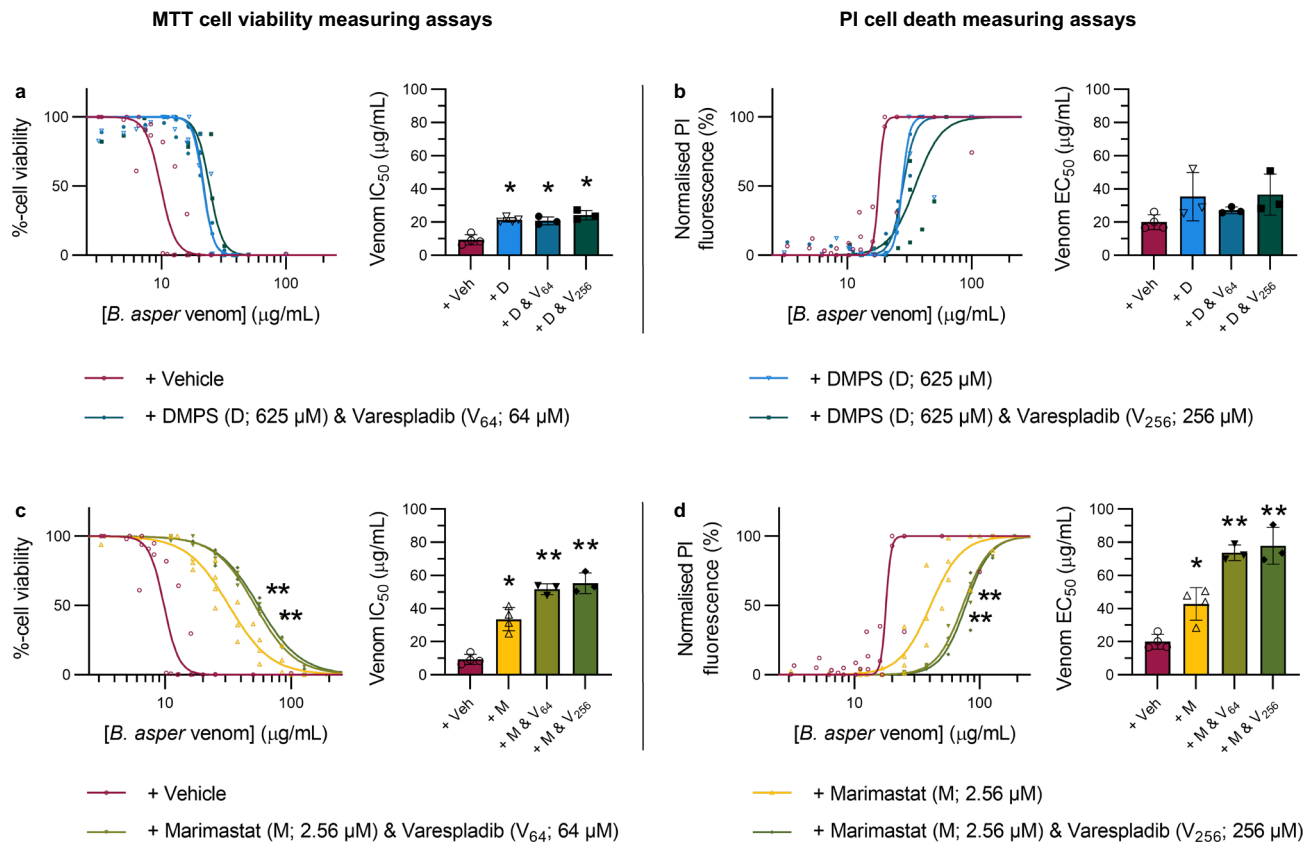


**Fig. 4 | Varespladib potentiates the inhibitory effects of marimastat, but not DMPS, against *B. asper* venom in HaCaT cells.** HaCaT cells were treated for 24 hours with serial dilutions of *B. asper* venom (2.2–190 μg/mL) that had been pre-incubated with drug vehicle control or with drug combination therapies consisting of DMPS (625 μM) plus varespladib (64 or 256 μM, abbreviated V<sub>64</sub> or V<sub>256</sub>, respectively; top row) or marimastat (2.56 μM) plus V<sub>64</sub> or V<sub>256</sub> (bottom row). For all treatment groups, MTT cell viability (LHS of figure) and PI cell death (RHS of figure) assays were performed. \* Signifies the value is significantly different than that of the vehicle control and \*\* signifies the value is significantly different than that of the

marimastat-alone treatment, as determined by a one-way ANOVA comparing all treatments to each other followed by Tukey's multiple comparisons test ( $P < 0.05$ ,  $n = 3$  [a]{D & V<sub>64</sub>, D & V<sub>256</sub>}, [b]{D, D & V<sub>64</sub>, D & V<sub>256</sub>}, [c]{M & V<sub>64</sub>, M & V<sub>256</sub>}, [d]{M & V<sub>64</sub>, M & V<sub>256</sub>}) or 4 [a]{Veh, D}, [b]{Veh, M}, [c]{Veh, M}, [d]{Veh, M} biologically independent cell experiments). ANOVA statistics for individual statistically analysed graphs are: **a**  $F(3,10) = 26.63$ ,  $P = 0.000044$ ; **b**  $F(3,9) = 2.382$ ,  $P = 0.1371$ ; **c**  $F(3,10) = 56.55$ ,  $P = 0.0000014$ ; **d**  $F(3,10) = 40.41$ ,  $P = 0.0000067$ . Data are presented as mean values  $\pm$  SD and the individual values for each trial are shown as points within each of the graphs. Source data are provided as a Source Data file.

decreased *E. ocellatus* venom-induced dermonecrosis in the dermis while DMPS and varespladib did not; no significant results were calculated from any treatment in any other skin layer (Supplementary Fig. 4d). While the mean overall dermonecrosis score induced by *E. ocellatus* venom was not significantly decreased by any treatment, there was a trend towards inhibition with DMPS, marimastat, DMPS and varespladib, and marimastat and varespladib resulting in mean overall dermonecrosis scores of 0.04, 0.00, 0.02, and 0.12, respectively, versus 1.04 for the drug-vehicle control and 0.74 for the varespladib treatment (Fig. 6g). Note that minimal necrosis was observed in the adventitia even in the absence of drug treatment, suggesting that histological scoring of necrosis in this layer is likely less informative than in other skin layers.

### The marimastat and varespladib drug combination inhibits the formation of dermal lesions by *B. asper* and *E. ocellatus* venoms when dosed up to one-hour post-venom

Although the *in vivo* preincubation model described above is an important first step for assessing the preclinical efficacy of snakebite treatments, it is limited in that venom and treatment are incubated together and co-administered, which does not accurately reflect a true snakebite treatment scenario<sup>64</sup>. To determine if it is possible for a SVMP- and PLA<sub>2</sub>-targeting drug combination therapy to inhibit dermal lesion formation post-venom, we next employed a 'rescue' or 'challenge-then-treat' experimental approach, where mice were ID-

challenged with venom from *B. asper* or *E. ocellatus* followed by a second ID-injection in the same location with the marimastat and varespladib combination therapy, either immediately (0 mins) or 5, 15 or 60 minutes later. The other conditions were as described for the preincubation model, with venom challenge and drug treatment doses the same and mice euthanised after 72 hours. Representative images and a full image set of the resulting dermal lesions are displayed in Fig. 7a and Supplementary Fig. 3, respectively. These experiments demonstrated that the efficacy of the marimastat and varespladib drug combination was retained in this more challenging model even when treatment was delayed for one hour, as significant reductions in the size of dermal lesions compared to the venom only controls were observed at every time point with both venoms (all comparisons  $P < 0.05$ ). For *B. asper*, venom-induced lesions decreased from a mean area of 22.4 to 0.6, 2.4, 5.8, and 6.6 mm<sup>2</sup> when treatment was dosed at 0, 5, 15 and 60 minutes, respectively (Fig. 7b), while those induced by *E. ocellatus* venom decreased from 14.1 to 0.6, 0.3, 0.0, and 6.1 mm<sup>2</sup>, respectively (Fig. 7c).

## Discussion

Antivenom remains the only currently available specific treatment for snakebite envenoming. Despite being lifesaving therapies, antivenoms have several limitations that hamper their clinical utility, and thus treatments with improved pan-snake species effectiveness, safety, and affordability are sorely needed<sup>9,37,38</sup>. Of particular importance is the

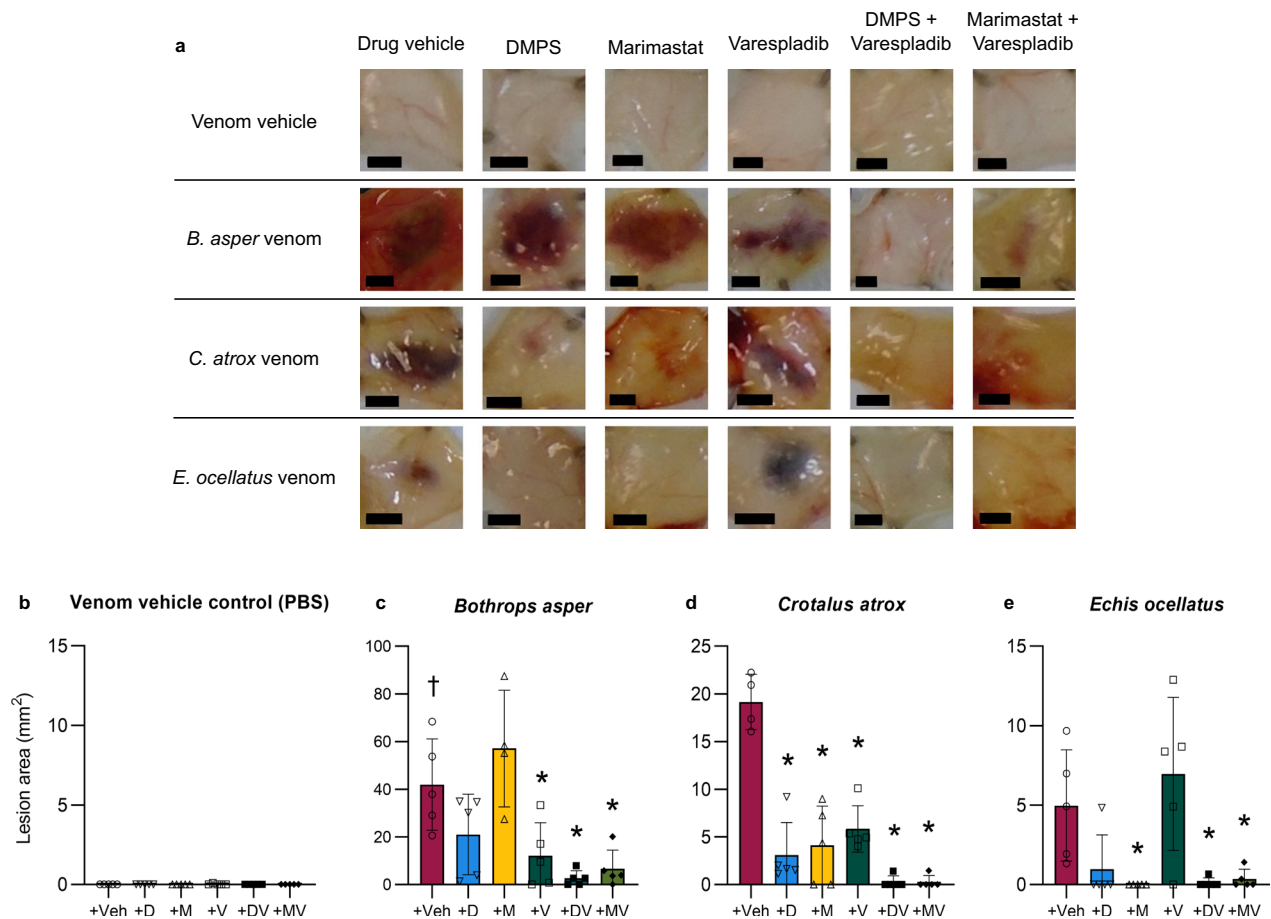


**Fig. 5 | Dermal lesions induced by distinct snake venoms are inhibited by drug combinations containing an SVMP and a PLA<sub>2</sub> inhibitor.** Individual mice were ID injected with *B. asper* (150 µg), *C. atrox* (100 µg), or *E. ocellatus* (39 µg) venom or venom vehicle control (PBS) that had been pre-incubated with drug vehicle control (98.48% PBS, 1.52% DMSO; Veh), DMPS (110 µg; D), marimastat (60 µg; M), varespladib (19 µg; V), DMPS & varespladib (110 and 19 µg, respectively; DV), or marimastat & varespladib (60 and 19 µg, respectively; MV). After 72 hours<sup>†</sup> the mice were euthanised and their lesions excised, height and width measured with callipers, and photographed. **a** Representative images of the lesions resulting from each treatment group (black scale bar represents 3 mm). Bar graphs summarising the average total lesion areas for each drug treatment group when pre-incubated with **b** venom vehicle control (PBS), **c** *B. asper*, **d** *C. atrox*, or **e** *E. ocellatus* venom. †

Signifies that these mice were culled at 24 h instead of the usual 72 h, due to their external lesions progressing to the maximum permitted size defined in our animal ethics licence, thus resulting in early euthanasia. \* Signifies that value is significantly different than that of the drug vehicle control for that venom as determined by a one-way ANOVA followed by Dunnett's multiple comparisons test ( $P < 0.05$ ,  $n = 4$  [c{M}, d{Veh}] or 5 [b{all}, c{Veh, D, V, DV, MV}, d{D, M, V, DV, MV}, e{all}] biologically independent animals). ANOVA statistics for individual statistically analysed graphs are: **b**  $F(5,24) = 1.000$ ,  $P = 0.4389$ , **c**  $F(5,23) = 8.808$ ,  $P = 0.000088$ ; **d**  $F(5,23) = 28.80$ ,  $P = 0.000000035$ ; **e**  $F(5,24) = 6.587$ ,  $P = 0.0005$ . Data are presented as mean values  $\pm$  SD and the individual values for each lesion are shown as points within each of the bars. Source data are provided as a Source Data file.

need to develop effective treatments for tackling snakebite-induced local tissue damage, for which current antivenoms are ineffective<sup>1,21–26</sup>. Due to their smaller size and pharmacological properties that could result in superior tissue distribution versus large antibodies, small molecule drugs may offer a more effective way of preventing morbidity-causing peripheral tissue damage around the bite-site that is typical of cytotoxic snakebite envenoming<sup>9,31,37–39</sup>. The properties of small molecule drugs could be exploited by developing oral snakebite therapies to be administered in the field immediately after a victim is bitten<sup>32</sup>, though the clinical success of this method for tackling local envenoming could be impeded due to the pharmacokinetic time lag associated with oral drugs<sup>65</sup> and the rapidity with which local swelling, blistering and/or tissue necrosis develop after cytotoxic snakebite<sup>1,25,36</sup>. Topical or locally injectable (i.e. transdermal) therapies administered immediately after a snakebite seem likely to overcome this weakness by directly and rapidly delivering the drugs to the exact location of need, as observed by the efficacy conferred via direct ID injection in our animal models (i.e. Figs. 5 and 7). Both subcutaneous and ID delivery of therapeutics/vaccines have been proven to be feasible in

resource poor settings<sup>66,67</sup> while delivery systems, such as microneedle devices or transdermal patches, are well established approaches for transdermal drug delivery<sup>41,68,69</sup>. Though local delivery of toxin inhibiting drugs seems likely to be of greatest benefit for tackling snakebite morbidity, both oral and transdermal delivery methods share the benefit of being amenable for rapid administration in the community soon after a snakebite occurs, and well before a patient could currently reach hospital for IV-administration of antivenom<sup>9,31,32,35,37–39</sup>. This is important when considering several studies have shown it can take on average 5–9 hours for a snakebite victim to reach hospital in rural, resource poor settings in which the burden of snakebite is greatest<sup>70–72</sup>.

In this study we sought to determine whether three toxin-inhibiting small molecule drugs (DMPS, marimastat, and varespladib), all of which have previously exhibited promising neutralising capabilities against snake venom-induced systemic effects<sup>29,32–34,36,44–49</sup>, were capable of preventing snake venom-induced dermonecrosis and thus might show promise for future translation as treatments of local tissue damage following snakebite envenoming. Cell-based cytotoxicity assays were completed as higher throughput and ethically

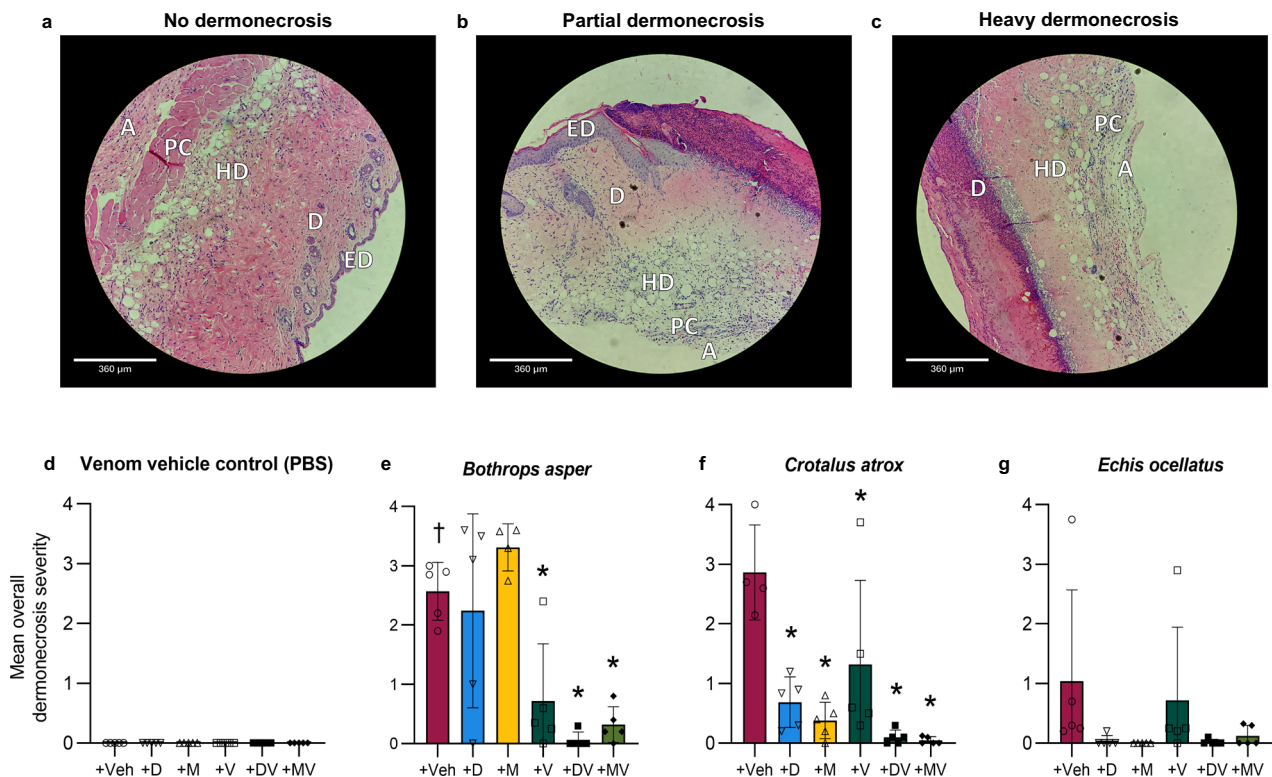


**Fig. 6 | Histopathological analysis of ID-injection site cross-sections confirms venom-induced dermonecrosis can be reduced using SVMP- and PLA<sub>2</sub>-inhibiting drugs.** Four  $\mu\text{m}$  H&E sections were prepared from formalin-fixed, paraffin-embedded tissue from dermal injection sites and photographed at 100X magnification. Two blinded and independent experimenters scored, between 0–4, the percentage of each skin layer that was necrotic (0 = 0%, 1 = 0–25%, 2 = 25–50%, 3 = 50–75%, and 4 = 75–100%). The highest recorded score per cross-section was used as a measure of the maximum severity reached within each skin sample. Representative 100X-magnified images showing **a** no dermonecrosis (mean overall dermonecrosis score of 0), **b** partial dermonecrosis (1.4) and **c** heavy dermonecrosis (2.4), with epidermis (ED), dermis (D), hypodermis (HD), panniculus carnosus (PC), and adventitia (A) annotated in each image (note that the ED is not visible in the ‘Heavy dermonecrosis’ image due to the severity of the ulceration, and was therefore given a necrosis score of 4). Bar graphs summarising the mean overall dermonecrosis severity scores in cross-sections from mice ID-injected with

**d** venom vehicle control (PBS), **e** *B. asper* venom, **f** *C. atrox* venom, or **g** *E. ocellatus* venom that had been pre-incubated with drug vehicle control (98.48% PBS, 1.52% DMSO; Veh), DMPS (110  $\mu\text{g}$ ; D), marimastat (60  $\mu\text{g}$ ; M), varespladib (19  $\mu\text{g}$ ; V), DMPS-plus-varespladib (110 and 19  $\mu\text{g}$ , respectively; DV), or marimastat-plus-varespladib (60 and 19  $\mu\text{g}$ , respectively; MV). † Signifies these mice were culled at 24 h instead of the usual 72 h, due to their external lesions progressing to the maximum permitted size defined in the animal ethics licence, resulting in early euthanasia. \* Signifies that value is significantly different than that of the drug vehicle control as determined by a one-way ANOVA followed by Dunnett’s multiple comparisons test ( $P < 0.05$ ,  $n = 4$  [e[M], f[Veh]] or 5 [d[all], e[Veh, D, V, DV, MV], f[D, M, V, DV, MV], g[all]] biologically independent animals). ANOVA statistics: **e**  $F(5,23) = 11.81$ ,  $P = 0.0000097$ ; **f**  $F(5, 23) = 10.30$ ,  $P = 0.000028$ ; **g**  $F(5,24) = 1.531$ ,  $P = 0.2178$ . Data are presented as mean values  $\pm$  SD and individual scores are shown as points within each of the figures’ bars. Source data are provided as a Source Data file.

acceptable alternatives to in vivo experiments for initial toxin-inhibitory experiments. The MTT assays<sup>50</sup> were used to detect two different effects of venoms on keratinocytes in culture, i.e., cell viability-inhibition and cellular detachment. Both effects are relevant in terms of the pathology induced by venoms in the skin. First, we determined the potency of a panel of geographically diverse and taxonomically distinct medically important snake species (both viperids and elapids) in HaCaT cells<sup>52,53</sup>, with resulting IC<sub>50</sub> values showing that most of the venoms (9 of the 11 tested) were equipotently cytotoxic (Fig. 1). These findings were unexpected given the extensive variation in toxin composition among these snake species<sup>10,73</sup>. As an additional pharmacological measure, the Hill slopes of all venoms were calculated and compared (Fig. 1m), and all 11 were greater than 1.5 and thus considered ‘steep’<sup>74</sup>, meaning a small change in venom concentration can lead to a large change in overall pathological effect. This finding suggests ‘positive cooperativity’<sup>55,56</sup> and probable pathological synergy between venom toxins, in line with previous findings<sup>75–77</sup>.

Our skin cell assays demonstrated that the SVMP-inhibitors DMPS and marimastat may be effective anti-cytotoxic drugs as individual therapies, although their inhibitory effects were not universal across all cytotoxic snake venoms (Fig. 2). Unexpectedly, the PLA<sub>2</sub> inhibitor

varespladib was ineffective against any of the venoms tested, despite it displaying impressive results against systemic venom-induced toxicity previously<sup>29,34,46–49</sup>. To explore whether MTT assays are simply a poor assay choice for testing PLA<sub>2</sub>-inhibitors against cytotoxic venoms, we multiplexed them with a secondary cytotoxicity assay using PI to measure cell membrane disruption<sup>59,60</sup>. Nevertheless, varespladib remained ineffective in these assays, suggesting that much of the cytotoxicity observed in these studies is mediated by SVMP toxins rather than PLA<sub>2</sub>s (Figs. 2 and 3); however, when we treated the cells with varespladib in combination with marimastat we observed significant reductions in the potency of *B. asper* venom versus the marimastat-alone treatment (Fig. 4). These findings suggest that PLA<sub>2</sub> toxins may indeed, at least to some extent, contribute to cytotoxic venom effects, and that combining an SVMP-inhibitor with a PLA<sub>2</sub>-inhibitor may improve overall treatment efficacy. Interestingly, this anti-cytotoxic potentiation of marimastat by varespladib was not observed with DMPS despite this drug also being a SVMP-inhibitor. This dichotomy is likely due to the mechanisms of action of these drugs being different, as marimastat directly inhibits metalloproteinases by acting as a peptidomimetic and binding covalently to the Zn<sup>2+</sup> ion present in the active site<sup>31,45,78–80</sup>, while the inhibitory mechanism of



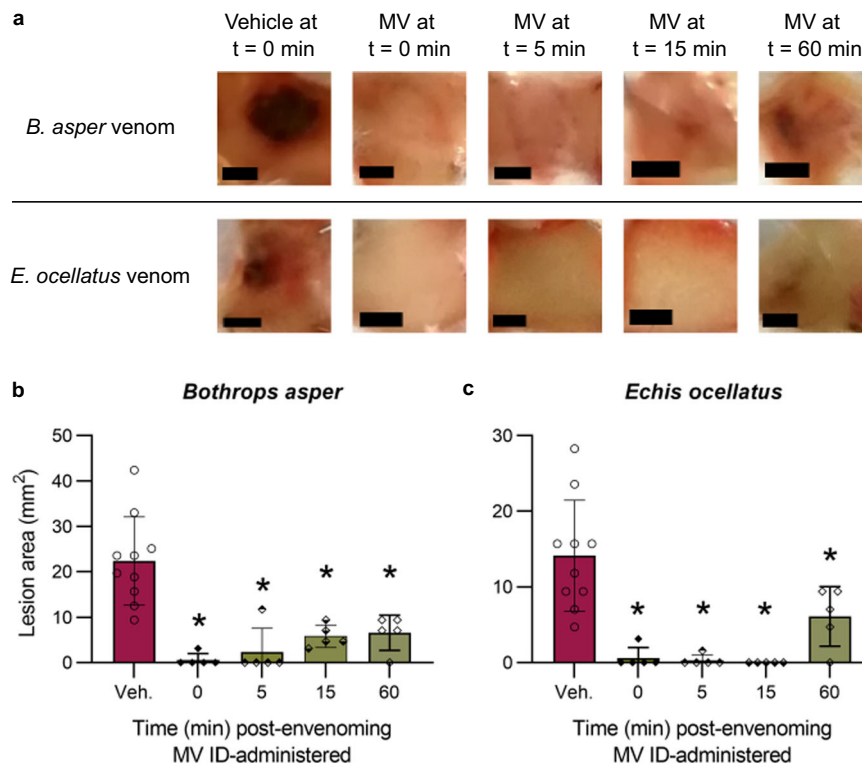


**Fig. 7 | The drug combination of marimastat and varespladib significantly inhibits the size of dermal lesions induced by *B. asper* and *E. ocellatus* venoms when delivered up to 1 hour after venom challenge.** Mice ( $n = 5$ ) were ID injected with *B. asper* (150 µg) or *E. ocellatus* (39 µg) venom and then ID injected in the same location at 0 minutes (i.e. a second injection immediately) post-venom challenge with drug vehicle control (98.48% PBS, 1.52% DMSO; Veh) or at 0-, 5-, 15-, or 60-minutes post-venom challenge with marimastat and varespladib (60 and 19 µg, respectively; MV). After 72 hours experimental animals were euthanised and their lesions excised, quantified, and photographed. **a** Representative images of the lesions resulting from each treatment group (black scale bar represents 3 mm). Bar

graphs summarising the ability of MV to inhibit skin lesion formation caused by **b** *B. asper* and **c** *E. ocellatus* venoms at 0-, 5-, 15-, and 60-minutes post-venom challenge. \* Signifies that value is significantly different than that of the drug vehicle control for that venom as determined by a one-way ANOVA followed by Dunnett's multiple comparisons test ( $P < 0.05$ ,  $n = 5$  [all drug treatments] or 10 [vehicle controls] biologically independent animals). ANOVA statistics for individual statistically analysed graphs are: **b**  $F(4,25) = 14.27$ ,  $P = 0.0000034$ , **c**  $F(4,25) = 12.88$ ,  $P = 0.00000795$ . Data are presented as mean values  $\pm$  SD and the individual values for each lesion are shown as points within each of the bars. Source data are provided as a Source Data file.

action of DMPS is solely the result of  $Zn^{2+}$  chelation<sup>32,78</sup>. These mechanistic variations likely underpin the previously described differences in SVMP-inhibiting potencies of these drugs in vitro<sup>33,81,82</sup>.

Using a drug pre-incubation<sup>32,33</sup> model of venom dermonecrosis in mice<sup>61</sup>, we next tested three venoms whose cytotoxic potencies were reduced by both DMPS and marimastat in the cell assays, and that were sourced from different genera that display considerable inter-species toxin variability<sup>10</sup> and inhabit distinct geographical regions (*B. asper*, Latin America; *C. atrox*, North America; *E. ocellatus*, West Africa) (Fig. 5). In line with the cell cytotoxicity findings, DMPS was effective against *C. atrox* venom-induced lesions and marimastat against both *C. atrox* and *E. ocellatus* venoms, likely due to the relatively high proportion of SVMPs in these two venoms<sup>10</sup>. However, contrasting with our cell data, neither SVMP-inhibitor reduced *B. asper* venom-induced lesion formation, suggesting the other toxins present in *B. asper* venom are sufficient to induce dermonecrosis in vivo. Also in contrast with our cellular results, the  $PLA_2$ -inhibiting drug varespladib was effective at inhibiting *B. asper* and *C. atrox* venoms in vivo, suggesting the inhibition of this single toxin family is sufficient to significantly reduce their overall dermonecrotic activity. These findings clearly evidence that cell-based cytotoxicity assays do not fully recapitulate findings obtained through in vivo dermonecrosis experiments, and that while DMPS, marimastat, and varespladib show efficacy in vivo, none are able to significantly reduce dermonecrosis caused by all three of these variable snake venoms as monotherapies.

Contrastingly, the two combination therapies tested (marimastat and varespladib, DMPS and varespladib) were both effective at

significantly reducing venom-induced dermonecrosis caused by the three tested venoms when co-administered with venom, and completely inhibited lesion formation in many of the experimental animals (Fig. 5, Supplementary Fig. 3). Histopathological analysis of the resulting lesions confirmed the efficacy of both drug combinations, with significant reductions observed in the severity scores of overall dermonecrosis measured throughout the various skin layers excised from mice envenomed with *B. asper* and *C. atrox* venoms (Fig. 6, Supplementary Fig. 4). These findings provide evidence of how a drug combination therapy that simultaneously inhibits both SVMP and  $PLA_2$  toxins provides increased snake species coverage over individual drugs for the prevention of in vivo local tissue damage caused by cytotoxic venoms. Finally, data generated from a rescue model of envenoming, where treatment was delivered after venom challenge, demonstrated that venom-induced dermonecrosis can be significantly inhibited by a dual drug combination even when treatment is delayed for up to an hour after envenoming (Fig. 7). These data suggest that locally injectable versions of a drug combination could be a viable treatment for snakebite victims to reduce the severity of cytotoxic effects, and that this treatment could significantly reduce life-altering symptoms even if the drug cannot be administered immediately after a bite.

When combined with the results of Albulescu, et al.<sup>33</sup>, our findings show that combination drug therapies simultaneously targeting SVMP and  $PLA_2$  toxins are likely to be useful for tackling both the life-threatening systemic and morbidity-causing local pathologies caused by diverse viperid snake venoms. Because snakebite is a global health

challenge that predominately affects populations in lower- and middle-income countries (LMICs), our findings here have considerable consequences for the future treatment of this WHO priority-listed NTD, particularly when considering that *E. ocellatus* are responsible for most snakebite deaths in West Africa<sup>83</sup>, with 9–13% of victims presenting with local skin blistering or necrosis<sup>84,85</sup>, and *B. asper* causes the vast majority of severe snakebites in Central America<sup>86</sup>, with more than a third of victims presenting with local tissue necrosis<sup>87</sup>. Further, evidence of inhibitory potential against *C. atrox*, a North American pit viper species responsible for causing severe local envenoming and a high incidence of tissue necrosis<sup>88</sup>, may enable a strategy for the future global translation of drug combination therapies by leveraging one of the few financially viable markets available for snakebite. Such an approach must, however, ensure that a robust access plan for LMIC communities is developed in parallel to avoid potential future distribution pitfalls, like those recently reported around the inequitable distribution of COVID vaccines<sup>89,90</sup>.

There remains much work to be done to translate these drugs and their combinations into approved snakebite therapies. This includes additional preclinical research, for example against the venoms of additional snake species (e.g. other viperids and cytotoxic *Naja* spitting cobras<sup>24,73,91</sup>), trials testing different routes of therapeutic administration<sup>32</sup>, and experiments to better understand their pharmacokinetics and pharmacodynamics to elucidate informed dosing regimens and potential drug-drug interactions. Since a major anticipated benefit of drug therapies for snakebite is their potential to be orally, topically, or transdermally formulated<sup>9</sup> (i.e. in contrast with intravenously-injected antivenom), considerable research effort should focus around this space to pursue the translation of safe, affordable, community-level interventions to reduce existing treatment delays in rural tropical communities, thus improving patient outcomes. To that end it is worth noting that DMPS is already undergoing Phase I clinical trials to determine both its safety and a PK-informed oral dosing regimen for snakebite indication<sup>92</sup>, while methyl varespladib has entered Phase II trials to assess its safety, tolerability, and efficacy in snakebite victims (<https://clinicaltrials.gov/ct2/show/NCT04996264>). These studies emphasise the growing confidence the research community has in specific small molecule drugs as treatments for snakebite envenoming, though the data presented here highlight that additional research to develop these (among other) drugs into combination therapies is likely to yield treatments with superior pan-snake species effectiveness than any single drug alone.

In conclusion, our data provide strong evidence that the small molecule drugs DMPS, marimastat, and varespladib can significantly protect against dermonecrosis associated with local snakebite envenoming, though their efficacy is limited to certain snake species. This limitation is largely overcome when the SVMP-inhibiting DMPS or marimastat are used in combination with the PLA<sub>2</sub>-inhibiting varespladib, most likely due to the dual role of SVMPs and PLA<sub>2</sub>s in the pathogenesis of tissue damage across snake species. Finally, we demonstrate that the efficacy of such a combination therapy is retained, even when the administration of the drug combination is delayed for one hour after venom challenge. Our findings therefore advocate for further research to help translate these drugs and their combinations into community-deliverable snakebite treatments with the goal of significantly reducing the morbidity associated with one of the world's most neglected tropical diseases.

## Methods

### Chemicals, drugs and biological materials

Thiazolyl blue methyltetrazolium bromide (MTT; M5655), dimethyl sulfoxide (DMSO; 276855), and propidium iodide (PI; P4170) were purchased from Sigma-Aldrich (Merck). Dulbecco's modified Eagle's medium (DMEM; 11574516), foetal bovine serum (FBS; 11573397),

FluoroBrite DMEM (A1896701), glutaMAX supplement (35050038), penicillin-streptomycin (11528876), phosphate buffered saline (11503387), and TrypLE Express were purchased from Gibco (Thermo Fisher Scientific). Marimastat (M2699) and varespladib (SML1100) were purchased from Sigma-Aldrich (Merck), and 2,3-dimercapto-1-propanesulfonic acid monohydrate (DMPS; H56578) was purchased from Alfa Aesar. Working stocks were: DMPS (PBS, 400 mM, made fresh with each use from lyophilised powder), marimastat (10 mM, ddH<sub>2</sub>O), and varespladib (65.7 mM, DMSO).

### Venoms

Venoms were sourced from either wild-caught snakes maintained, or historical venom samples stored, in the herpetarium of the Centre for Snakebite Research & Interventions at the Liverpool School of Tropical Medicine (LSTM). This facility and its protocols for the husbandry of snakes are approved and inspected by the UK Home Office and the LSTM and University of Liverpool Animal Welfare and Ethical Review Boards. The venom pools were from snakes with diverse geographic localities, namely: *Bitis arietans* (Nigeria), *Bothrops asper* (Costa Rica [Caribbean region]), *Crotalus atrox* (captive bred [USA lineage]), *Calloselasma rhodostoma* (Malaysia), *Daboia russelii* (Sri Lanka), *Echis carinatus* (India), *Echis ocellatus* (Nigeria [likely *Echis romani* following recent taxonomic reclassification, but awaiting species genotyping confirmation]), *Naja haje* (Uganda), East-African *Naja nigricollis* (Tanzania), West-African *Naja nigricollis* (Nigeria), and *Naja pallida* (Tanzania). Note that the Indian *E. carinatus* venom was collected from a specimen that was inadvertently imported to the UK via a boat shipment of stone, and then rehoused at LSTM on the request of the UK Royal Society for the Prevention of Cruelty to Animals (RSPCA). Crude venoms were lyophilized and stored at 4 °C to ensure long-term stability. Prior to use, venoms were resuspended to 10 mg/ml in PBS and then kept at –80 °C until used in the described experiments, with freeze-thaw cycles kept to a minimum to prevent degradation.

### Cells

The immortalised human epidermal keratinocyte line, HaCaT<sup>52,53</sup>, was purchased from Caltag Medsystems (Buckingham, UK) and supplied by AddexBio (San Diego, USA): Catalogue number T0020001, and authenticated by AddexBio using STR profiling. Cells were cultured in phenol red-containing DMEM with GlutaMAX supplemented with 10% FBS, 100 IU/mL penicillin, 250 µg/mL streptomycin, and 2 mM sodium pyruvate (standard medium; Gibco) per Caltag's HaCaT protocol. For assays that contained the fluorescent dye, PI, a medium specifically formulated for fluorescence-based cell assays was used instead: FluoroBrite DMEM supplemented with 1% GlutaMAX 100x supplement, 1% FBS, 100 IU/mL penicillin, 250 µg/mL streptomycin, and 2 mM sodium pyruvate (minimally fluorescent medium; Gibco). The cells were split and growth medium changed 2x per week up to a maximum of 30 passages. Cells were maintained in a humidified, 95% air/5% CO<sub>2</sub> atmosphere at 37 °C (standard conditions).

### MTT cell viability and PI cell death assays

MTT assays were used to evaluate the cell (HaCaT) viability-inhibiting activity of snake venoms and high concentrations of drug inhibitors and were based on the methods of Issa, et al.<sup>93</sup>. PI assays were used to evaluate the cell death and were based on the methods of Chitolie & Toescu<sup>60</sup>.

**MTT assays alone.** HaCaT cells were seeded (5,000 cells/well, clear-sided 96-well plates) in standard medium, then left to adhere overnight at standard conditions. The next day, serial dilutions were prepared in standard medium of (a) venom treatments (1–1,024 µg/mL; i.e. Fig. 1), (b) DMPS (9.8–10,000 µM), marimastat (0.04–40.96 µM), or varespladib (1–1,024 µM) treatments (i.e. Supplementary Fig. 1), or (c)

venoms (2.5–240 µg/mL) preincubated with a single concentration (the  $MTC_{1/2}$  as determined in b) of DMPS (625 µM), marimastat (2.56 µM), varespladib (128 µM) or drug vehicle control at standard conditions for 30 minutes (i.e. Fig. 2). Cells were treated with each prepared solution (100 µL/well, triplicate wells/prepared solution) for 24 hours. Thereafter, MTT solution (3.33 mg/mL) was prepared in PBS, filtered through a 0.22 µm syringe filter, then 30 µL added to each treatment well (and to 'no treatment' positive control wells and 'no cell' negative control wells) creating a final MTT concentration of 0.833 mg/mL. The plates were then incubated for 1.5 h at standard conditions for the MTT reaction to occur, after which medium was aspirated from all wells and replaced with 100 µL of DMSO. Plates were shaken to ensure a homogenous mixture of purple formazan, and then absorbance (550 nm;  $A_{550}$ ) read on a FLUOstar Omega Microplate Reader. The % adherent cell viability for each treatment well was calculated as follows:

$$\% \text{ cell viability} = \frac{A_{550 \text{ treatment well}} - \text{Average}(A_{550 \text{ blank wells}})}{\text{Average}(A_{550 \text{ positive control wells}}) - \text{Average}(A_{550 \text{ blank wells}})} \times 100\% \quad (1)$$

The concentration that resulted in a 50% reduction in adherent cell viability ( $IC_{50}$ ) was calculated from the  $\log_{10}$  concentration versus normalised response curves using the 'log(inhibitor) vs. normalized response - Variable slope' in GraphPad Prism, which uses the following equation:

$$y = \frac{100}{1 + 10^{(\text{Log}IC_{50} - x)\text{HillSlope}}} \quad (2)$$

where  $y$  is the normalised %-cell viability values and  $x$  is the  $\log_{10}$  of the venom concentrations.

**MTT assays multiplexed with PI assays.** HaCaT cells were seeded (20,000 cells/well, black-sided & clear-bottomed 96-well plates) in standard medium, then left to adhere overnight at standard conditions. The next day, serial dilutions of *D. russelii* or *B. asper* venom (2.2–127 µg/mL) with a single concentration of DMPS (625 µM), marimastat (2.56 µM), varespladib (256 µM), DMPS & varespladib (DV; 625 µM and 256 µM, respectively), marimastat & varespladib (MV; 2.56 µM and 256 µM, respectively) or drug vehicle control (i.e. Figs. 3 and 4) were prepared in minimally fluorescent medium supplemented with 74.8 µM (50 µg/mL) PI and pre-incubated at standard conditions for 30 minutes prior to cell exposure. After pre-incubation, cells were treated with each prepared solution (100 µL/well, triplicate wells/prepared solution). After 24 h, PI fluorescence ( $EX_{544}/EM_{612}$ , read from bottom of plate at multiple points within each well) was read on a FlexStation 3 Multi-Mode Microplate Reader (Molecular Devices). PI relative fluorescence units (RFUs) of each treatment minus those of the PI solution blanks (no cells) were recorded as a measure of cell death and normalised between 0–100 to create PI dose-response curves. The venom dose at which the normalised PI reading was 50% of each treatment's maximum (the half maximal effective concentration, or  $EC_{50}$  value) was determined using the 'log(agonist) vs. normalized response - Variable slope' in GraphPad Prism, which uses the following equation:

$$y = \frac{100}{1 + 10^{(\text{Log}EC_{50} - x)\text{HillSlope}}} \quad (3)$$

where  $y$  is the normalised PI ( $RFU_{\text{treatment}} \text{ minus } RFU_{\text{blanks}}$ ) values and  $x$  is the  $\log_{10}$  of the venom concentrations. After the PI assays were completed, the PI-containing treatment solutions were aspirated from each well and replaced with 100 µL/well of minimally fluorescent medium containing 0.833 mg/mL of filtered MTT solution, and MTT assays completed and analysed as described above.

## Animal ethics and maintenance

Liverpool, UK: All 'drug preincubation' animal experiments (Figs. 5 and 6) were conducted using protocols approved by the Animal Welfare and Ethical Review Boards of the Liverpool School of Tropical Medicine and the University of Liverpool and were performed in pathogen-free conditions under licensed approval (PPL #P58464F90) of the UK Home Office and in accordance with the Animal [Scientific Procedures] Act 1986 and institutional guidance on animal care. All experimental animals (18–20 g [4–5 weeks old], male, CD-1 mice, Charles River, UK) were acclimatised for a minimum of one week before experimentation with their health monitored daily. Mice were grouped in cages of five, with room conditions of approximately 22 °C at 40–50% humidity, with 12/12 hour light cycles, and given ad lib access to CRM irradiated food (Special Diet Services, UK) and reverse osmosis water in an automatic water system. Mice were housed in specific-pathogen free facilities in Techniplast GM500 cages containing Lignocell bedding (JRS, Germany), Sizzlenest zigzag fibres as nesting material (RAJA), and supplied with environmental enrichment materials. San José, Costa Rica: All 'rescue' animal experiments (Fig. 7) were conducted using protocols approved by the Institutional Committee for the Care and Use of Laboratory Animals (CICUA) of the University of Costa Rica (approval number CICUA 82-08). All experimental animals (18–20 g [4–5 weeks old], mixed sex, CD-1 mice, Instituto Clodomiro Picado, Costa Rica) were acclimatised for a minimum of one week before experimentation, with their health monitored daily. Mice were grouped in cages of five, with room conditions of approximately 22–24 °C at 60–65% humidity, with 12/12 hour light cycles, and given ad lib access to food and water, and housed in Techniplast Eurostandard Type II 1264 C cages.

## Preclinical anti-dermonecrosis efficacy of small molecule drugs via a preincubation model of envenoming

The in vivo experimental design was based upon 3R-refined WHO-recommended envenoming protocols<sup>32,61</sup>, with animals randomised and observers being blinded to the drug and vehicle treatments, and the anti-dermonecrosis methods were based on the Minimum Necrotizing Dose (MND) principles originally described in Theakston and Reid<sup>61</sup>. Before commencing the drug trials, appropriate necrotic doses of *B. asper* and *C. atrox* venom-alone were determined. Groups of two-to-three mice received ID injections in the shaved rear quadrant on the dorsal side of their flank skin with 50 µL treatments containing *B. asper* (50, 75, 100, 150, 200, or 250 µg) or *C. atrox* (30.5, 50, 75, 100, 150, or 200 µg) venom. The most appropriate experimental doses were those that consistently induced visible external lesions that grew to no more than 10 mm in diameter without inducing signs of systemic envenoming, as stipulated by our ethics licencing; these were determined to be 150 µg of *B. asper* venom and 100 µg of *C. atrox* venom (i.e. Supplementary Fig. 2). The 39 µg dose for *E. ocellatus* venom was previously published<sup>62</sup>. For anti-dermonecrosis small molecule drug trials, groups of five mice received experimental doses per mouse that consisted of: (a) venom alone, (b) venom plus drug (DMPS, marimastat, varespladib, DMPS plus varespladib [DV], or marimastat plus varespladib [MV]), or (c) venom vehicle (PBS) plus drug. Albuлесcu, et al. previously used 60 µg/mouse of marimastat in their preclinical ID haemotoxicity trials<sup>33</sup>, therefore this same marimastat dose was chosen for our dermonecrosis trials. A slightly higher dose of DMPS (110 µg/mouse) was chosen due to our findings that DMPS is a less potent inhibitor of cytotoxicity than marimastat in HaCaT cells, and a lower dose of varespladib (19 µg/mouse) was chosen due to solubility issues at higher drug concentrations. Stock solutions of DMPS and marimastat were dissolved in PBS, while the more hydrophobic varespladib was dissolved in DMSO; therefore, for the sake of inter-treatment consistency the same drug-vehicle control was used within all treatments described above, which

resulted in a final treatment vehicle solution of 1.52% DMSO and 98.48% PBS. All experimental doses were prepared to a volume of 50  $\mu$ L and incubated at 37 °C for 30 minutes, then kept on ice for no more than 3 hours until the mice were injected. For dose delivery, mice were briefly anaesthetised using inhalational isoflurane (4% for induction of anaesthesia, 1.5–2% for maintenance) and ID-injected in the shaved rear quadrant on the dorsal side of the flank skin with the 50  $\mu$ L treatments. The mice were observed three times daily up to 72 hours post-injection to check for symptoms of systemic envenoming or excessive external lesion development, which would have necessitated early termination of the animal due to reaching a humane endpoint defined by the animal ethics licence. At the end of the experiments (72 hours, except for the single group of *B. asper* venom plus drug vehicle control-treated mice that experienced greater-than-anticipated lesion development for which the time point was 24 hours), the mice were euthanised using rising concentrations of CO<sub>2</sub>, after which the skin surrounding the injection site was dissected and internal skin lesions measured with callipers and photographed. Cross-sections of the skin lesions were further dissected and preserved in formalin for mounting on microscopy slides for downstream histopathological analysis.

### Preparation and histopathological analysis of H&E-stained sections of venom-induced lesions

Skin samples underwent tissue processing using a Tissue-Tek VIP (vacuum infiltration processor) overnight before being embedded in paraffin (Ultraplast premium embedding medium, Solmedia, WAX060). Next, 4  $\mu$ m paraffin sections were cut on a Leica RM2125 RT microtome, floated on a water bath and placed on colour slides (Solmedia, MSS54511YW) or poly-lysine slides (Solmedia MSS61012S) to dry. For haematoxylin & eosin (H&E) staining, slides were dewaxed in xylene and rehydrated through descending grades of ethanol (100%, 96%, 85%, 70%) to distilled water before being stained in haematoxylin for 5 mins, “blued” in tap water for 5 mins, then stained in eosin for 2 mins. Slides were then dehydrated through 96% and 100% ethanol to xylene and cover slipped using DPX (Cellpath SEA-1304-00A). Haematoxylin (Atom Scientific, RRBD61-X) and Eosin (TCS, HS250) solutions were made up in house. Brightfield images of the H&E-stained lesions were taken with an Echo Revolve microscope (Settings: 100x magnification; LED: 100%; Brightness: 30; Contrast: 50; Colour balance: 50), with at least five images taken per cross-section. Histologic evidence of necrosis was assessed separately for the epidermis, dermis, hypodermis, panniculus carnosus, and adventitia. Features of necrosis included loss of nuclei, nuclear fragmentation (karyorrhexis), nuclear shrinkage and hyperchromasia (pyknosis), loss of cytoplasmic detail with hypereosinophilia, loss of cell borders, and, in the case of severe necrosis, disarray with complete loss of architecture and hyalinization. In the epidermis, ulceration with superficial debris was interpreted as evidence of necrosis. In the dermis, loss of skin adnexal structures (e.g. hair follicles and sebaceous glands) and extracellular matrix disarray were also interpreted as evidence of necrosis. Expanding upon methods originally published by Ho, et al.<sup>63</sup>, the %-necrosis of each skin layer (epidermis, dermis, hypodermis, panniculus carnosus, and adventitia) within each image was assessed by two independent and blinded pathologists and scored between a 0 and 4, with a 0 meaning no observable necrosis in the layer within that image, a 1 meaning up to 25% of the layer in that image exhibiting signs of necrosis, a 2 meaning 25–50% necrosis, a 3 meaning 50–75%, and a 4 meaning more than 75% exhibiting indicators of necrosis. The mean scores of the pathologists for each layer from each image were determined, and the highest scores-per-mouse used for our data analysis as these represented the maximum necrotic severity within each lesion (i.e. Supplementary Fig. 4). The ‘mean overall dermonecrosis severity’ was determined for each lesion by taking the mean of the individual layer scores (i.e. Fig. 6d–g).

### Preclinical anti-dermonecrosis efficacy of small molecule drug combinations via a ‘rescue’ model of envenoming

Groups of five mice were pre-treated with the analgesic tramadol (50 mg/kg by the subcutaneous route). Fifteen minutes later, mice were ID-injected with venom from either *B. asper* (150  $\mu$ g) or *E. ocellatus* (39  $\mu$ g) diluted in 25  $\mu$ L of PBS, and then immediately ( $t = 0$  min) ID-injected with 25  $\mu$ L of drug vehicle (3.04% DMSO and 96.96% PBS) or with a combination of marimastat (60  $\mu$ g) and varespladib (19  $\mu$ g) dissolved in 25  $\mu$ L of drug vehicle at 0, 5, 15, and 60 minutes post-envenoming. After 72 hours mice were euthanised by CO<sub>2</sub> inhalation, the skin surrounding the injection site was dissected, and the internal necrotic lesions were measured and photographed as described above.

### Statistical analysis

All data are presented as mean  $\pm$  standard deviation<sup>94</sup> of at least three independent experimental replicates. For cell experiments, ‘n’ is defined as an independent experiment completed at a separate time from other ‘n’s within that group of experiments; all drug and/or venom treatments within an ‘n’ were completed in triplicate wells and the mean taken as the final value for that one trial. For in vivo experiments, ‘n’ is defined as the number of mice in that specific treatment group<sup>95</sup>. Two-tailed *t*-tests were performed for dual comparisons, one-way analysis of variances (ANOVAs) performed for multiple comparisons with one independent variable followed by Dunnett’s or Tukey’s multiple comparisons tests when the trial data were compared to a single control group or to all other groups, respectively, as recommended by GraphPad Prism, and two-way ANOVAs performed for multiple comparisons with two independent variables followed by Dunnett’s multiple comparisons tests. A difference was considered significant if  $P \leq 0.05$ .

### Reporting summary

Further information on research design is available in the Nature Portfolio Reporting Summary linked to this article.

### Data availability

There are no restrictions on data availability. The H&E-stained dermal cross-sections of murine tissue used for histopathological analysis have been deposited in the Figshare database under accession code: 10.6084/m9.figshare.19706761.v1<sup>96</sup>. Source data are provided with this paper.

### References

- Gutiérrez, J. M. et al. Snakebite envenoming. *Nat Rev Dis Primers* **3**, 1–21 (2017).
- Kasturiratne, A. et al. The global burden of snakebite: a literature analysis and modelling based on regional estimates of envenoming and deaths. *PLoS Med* **5**, 1591–1604 (2008).
- Longbottom, J. et al. Vulnerability to snakebite envenoming: a global mapping of hotspots. *Lancet* **392**, 673–684 (2018).
- Waidyanatha, S., Silva, A., Siribaddana, S. & Isbister, G. K. Long-term effects of snake envenoming. *Toxins* **11**, 1–13 (2019).
- Molyneux, D. H. The London declaration on neglected tropical diseases: 5 years on. *Trans. R Soc. Trop. Med. Hyg.* **110**, 623–625 (2016).
- Annan, K. Snakebite: the biggest public health crisis you’ve never heard of. <https://www.kofiannanfoundation.org/combating-hunger/public-health-snakebite/> (2018).
- Williams, D. J. et al. Strategy for a globally coordinated response to a priority neglected tropical disease: snakebite envenoming. *PLoS Negl. Trop. Dis.* **13**, 1–12 (2019).
- Casewell, N. R., Jackson, T. N. W., Laustsen, A. H. & Sunagar, K. Causes and consequences of snake venom variation. *Trends Pharmacol. Sci.* **41**, 570–581 (2020).

9. Clare, R. H., Hall, S. R., Patel, R. N. & Casewell, N. R. Small molecule drug discovery for neglected tropical snakebite. *Trends Pharmacol. Sci.* **42**, 340–353 (2021).
10. Tasoulis, T. & Isbister, G. K. A review and database of snake venom proteomes. *Toxins* **9**, 1–23 (2017).
11. Slagboom, J., Kool, J., Harrison, R. A. & Casewell, N. R. Haemotoxic snake venoms: their functional activity, impact on snakebite victims and pharmaceutical promise. *Br. J. Haematol.* **177**, 947–959 (2017).
12. Ferraz, C. R. et al. Multifunctional toxins in snake venoms and therapeutic implications: from pain to hemorrhage and necrosis. *Front. Ecol. Evol.* **7**, 1–19 (2019).
13. Gutiérrez, J. M., Escalante, T., Rucavado, A. & Herrera, C. Hemorrhage caused by snake venom metalloproteinases: a journey of discovery and understanding. *Toxins* **8**, 1–19 (2016).
14. Ranawaka, U. K., Laloo, D. G. & de Silva, H. J. Neurotoxicity in snakebite - the limits of our knowledge. *PLoS Negl. Trop. Dis.* **7**, 1–18 (2013).
15. Fujioka, M. Skin necrosis due to snakebites. in *Skin Necrosis* (eds. Téot, L., Meaume, S., Ennis, W. & del Marmol, V.) 109–115 (Springer-Verlag Wien, 2015).
16. Chakrabarty, D. & Sarkar, A. Cytotoxic effects of snake venoms. in *Snake Venoms* (eds. Gopalakrishnakone, P., Inagaki, H., Vogel, C.-W., Mukherjee, A. K. & Rahmy, T. R.) 1–16 (Springer, 2016).
17. Brown, N. & Landon, J. Antivenom: the most cost-effective treatment in the world? *Toxicon* **55**, 1405–1407 (2010).
18. de Silva, H. A., Ryan, N. M. & de Silva, H. J. Adverse reactions to snake antivenom, and their prevention and treatment. *Br. J. Clin. Pharmacol.* **81**, 446–452 (2016).
19. Laloo, D. G. & Theakston, R. D. G. Snake antivenoms. *J. Toxicol. Clin. Toxicol.* **41**, 277–290 (2003).
20. Harrison, R. A. et al. Preclinical antivenom-efficacy testing reveals potentially disturbing deficiencies of snakebite treatment capability in East Africa. *PLoS Negl. Trop. Dis.* **11**, 1–24 (2017).
21. Kini, R. M., Sidhu, S. S. & Laustsen, A. H. Biosynthetic oligoclonal antivenom (BOA) for snakebite and next-generation treatments for snakebite victims. *Toxins* **10**, 1–10 (2018).
22. Mao, Y. C. et al. *Naja atra* snakebite in Taiwan. *Clin. Toxicol.* **56**, 273–280 (2017).
23. Lin, C. C., Chaou, C. H. & Gao, S. Y. Influential factors of local tissue necrosis after Taiwan cobra bites: A secondary analysis of the clinical significance of venom detection in patients of cobra snakebites. *Toxins* **13**, 1–11 (2021).
24. Rivel, M. et al. Pathogenesis of dermonecrosis induced by venom of the spitting cobra, *Naja nigricollis*: an experimental study in mice. *Toxicon* **119**, 171–179 (2016).
25. Liu, C. C. et al. Pathogenesis of local necrosis induced by *Naja atra* venom: Assessment of the neutralization ability of Taiwanese freeze-dried neurotoxic antivenom in animal models. *PLoS Negl. Trop. Dis.* **14**, 1–20 (2020).
26. Ferreira Junior, R. S. & Barraviera, B. Tissue necrosis after canine bothropic envenoming: a case report. *J. Venom. Anim. Toxins* **7**, 302–312 (2001).
27. Laustsen, A. H., Johansen, K. H., Engmark, M. & Andersen, M. R. Recombinant snakebite antivenoms: a cost-competitive solution to a neglected tropical disease? *PLoS Negl. Trop. Dis.* **11**, 1–14 (2017).
28. Laustsen, A. H. How can monoclonal antibodies be harnessed against neglected tropical diseases and other infectious diseases? *Expert. Opin. Drug Discov.* **14**, 1103–1112 (2019).
29. Lewin, M., Samuel, S., Merkel, J. & Bickler, P. Varespladib (LY315920) appears to be a potent, broad-spectrum, inhibitor of snake venom phospholipase A2 and a possible pre-referral treatment for envenomation. *Toxins* **8**, 1–16 (2016).
30. Wang, Y. et al. Exploration of the inhibitory potential of varespladib for snakebite envenomation. *Molecules* **23**, 1–13 (2018).
31. Layfield, H. J. et al. Repurposing cancer drugs batimastat and marimastat to inhibit the activity of a group I metalloprotease from the venom of the western diamondback rattlesnake, *Crotalus atrox*. *Toxins* **12**, 1–17 (2020).
32. Albulescu, L.-O. et al. Preclinical validation of a repurposed metal chelator as a community-based therapeutic for hemotoxic snakebite. *Sci. Transl. Med.* **12**, 1–13 (2020).
33. Albulescu, L.-O. et al. A therapeutic combination of two small molecule toxin inhibitors provides broad preclinical efficacy against viper snakebite. *Nat. Commun.* **11**, 1–14 (2020).
34. Xie, C. et al. Neutralizing effects of small molecule inhibitors and metal chelators on coagulopathic Viperinae snake venom toxins. *Biomedicines* **8**, 1–18 (2020).
35. Bulfone, T. C., Samuel, S. P., Bickler, P. E. & Lewin, M. R. Developing small molecule therapeutics for the initial and adjunctive treatment of snakebite. *J. Trop. Med.* **2018**, 1–10 (2018).
36. Rucavado, A. et al. Inhibition of local hemorrhage and dermonecrosis induced by *Bothrops asper* snake venom: effectiveness of early in situ administration of the peptidomimetic metalloproteinase inhibitor batimastat and the chelating agent CaNa2EDTA. *Am. J. Trop. Med. Hyg.* **63**, 313–319 (2000).
37. Williams, D. et al. The global snake bite initiative: an antidote for snake bite. *Lancet* **375**, 89–91 (2010).
38. Williams, H. F. et al. The urgent need to develop novel strategies for the diagnosis and treatment of snakebites. *Toxins* **11**, 1–29 (2019).
39. Benson, H. A. E., Grice, J. E., Mohammed, Y., Namjoshi, S. & Roberts, M. S. Topical and transdermal drug delivery: from simple potions to smart technologies. *Curr. Drug Deliv.* **16**, 444–460 (2019).
40. Alkilani, A. Z., McCrudden, M. T. C. & Donnelly, R. F. Transdermal drug delivery: Innovative pharmaceutical developments based on disruption of the barrier properties of the stratum corneum. *Pharmaceutics* **7**, 438–470 (2015).
41. Tiwari, N., Aggarwal, G., Jain, G. K. & Mittal, G. Multi-drug loaded microneedles for emergency treatment of snakebite envenomation. *Med. Hypotheses* **165**, 1–7 (2022).
42. Nicholls, S. J. et al. Varespladib and cardiovascular events in patients with an acute coronary syndrome: the VISTA-16 randomized clinical trial. *J. Am. Med. Assoc.* **311**, 252–262 (2014).
43. Winer, A., Adams, S. & Mignatti, P. Matrix metalloproteinase inhibitors in cancer therapy: turning past failures into future successes. *Mol. Cancer Ther.* **17**, 1147–1155 (2018).
44. Arias, A. S., Rucavado, A. & Gutiérrez, J. M. Peptidomimetic hydroxamate metalloproteinase inhibitors abrogate local and systemic toxicity induced by *Echis ocellatus* (saw-scaled) snake venom. *Toxicon* **132**, 40–49 (2017).
45. Howes, J.-M., Theakston, R. D. G. & Laing, G. D. Neutralization of the haemorrhagic activities of viperine snake venoms and venom metalloproteinases using synthetic peptide inhibitors and chelators. *Toxicon* **49**, 734–739 (2007).
46. Bryan-Quirós, W., Fernández, J., Gutiérrez, J. M., Lewin, M. R. & Lomonte, B. Neutralizing properties of LY315920 toward snake venom group I and II myotoxic phospholipases A2. *Toxicon* **157**, 1–7 (2019).
47. Lewin, M. et al. Delayed Oral LY333013 Rescues Mice from Highly Neurotoxic, Lethal Doses of Papuan Taipan (*Oxyuranus scutellatus*) Venom. *Toxins* **10**, 380 (2018).
48. Lewin, M. et al. Delayed LY333013 (oral) and LY315920 (intravenous) reverse severe neurotoxicity and rescue juvenile pigs from lethal doses of *Micrurus fulvius* (Eastern coral snake) venom. *Toxins* **10**, 1–17 (2018).
49. Gutiérrez, J. M., Lewin, M. R., Williams, D. J. & Lomonte, B. Varespladib (LY315920) and methyl varespladib (LY333013) abrogate or delay lethality induced by presynaptically acting neurotoxic snake venoms. *Toxins* **12**, 1–12 (2020).

50. Mosmann, T. Rapid colorimetric assay for cellular growth and survival: application to proliferation and cytotoxicity assays. *J. Immunol. Methods* **65**, 55–63 (1983).
51. Riss, T. L. et al. Cell viability assays [2016 edited version]. in *Assay Guidance Manual* (eds. Sittampalam, G. S. et al.) 295–320 (Eli Lilly & Company and the National Center for Advancing Translational Sciences, 2013).
52. Colombo, I. et al. HaCaT cells as a reliable in vitro differentiation model to dissect the inflammatory/repair response of human keratinocytes. *Mediat. Inflamm* **2017**, 1–12 (2017).
53. Wilson, V. G. Growth and differentiation of HaCaT keratinocytes. *Methods Mol. Biol.* **1195**, 33–41 (2014).
54. Borkow, G., Gutiérrez, J. & Ovidia, M. In vitro activity of BaH1, the main hemorrhagic toxin of *Bothrops asper* snake venom on bovine endothelial cells. *Toxicon* **33**, 1387–1391 (1995).
55. Fallahi-Sichani, M., Honarnejad, S., Heiser, L. M., Gray, J. W. & Sorger, P. K. Metrics other than potency reveal systematic variation in responses to cancer drugs. *Nat. Chem. Biol.* **9**, 708–714 (2013).
56. Black, J. A personal view of pharmacology. *Annu. Rev. Pharmacol. Toxicol.* **36**, 1–33 (1996).
57. Hall, S. R. et al. A lipid-based oral supplement protects skin cells in culture from ultraviolet light and activates antioxidant and anti-inflammatory mechanisms. *J. Natural Health Product Res.* **2**, 1–14 (2020).
58. Corkery, D. P., Dellaire, G. & Berman, J. N. Leukaemia xenotransplantation in zebrafish – chemotherapy response assay in vivo. *Br. J. Haematol.* **153**, 786–789 (2011).
59. Chiaraviglio, L. & Kirby, J. E. Evaluation of impermeant, DNA-binding dye fluorescence as a real-time readout of eukaryotic cell toxicity in a high throughput screening format. *Assay Drug Dev. Technol.* **12**, 219–228 (2014).
60. Chitolie, M. S. & Toescu, E. C. High-throughput method for dynamic measurements of cellular viability using a FLUOstar OPTIMA. *BMG LABTECH* vol. 04 1–2 <https://www.bmglabtech.com/high-throughput-method-for-dynamic-measurements-of-cellular-viability-using-a-bmg-labtech-microplate-reader/> (2008).
61. Theakston, R. D. & Reid, H. A. Development of simple standard assay procedures for the characterization of snake venom. *Bull World Health Organ* **61**, 949–956 (1983).
62. Segura, Á. et al. Preclinical assessment of the efficacy of a new antivenom (EchiTab-Plus-ICP®) for the treatment of viper envenoming in sub-Saharan Africa. *Toxicon* **55**, 369–374 (2010).
63. Ho, C. H. et al. Analysis of the necrosis-inducing components of the venom of *Naja atra* and assessment of the neutralization ability of freeze-dried antivenom. *Toxins* **13**, 1–12 (2021).
64. Knudsen, C. et al. Novel Snakebite Therapeutics Must Be Tested in Appropriate Rescue Models to Robustly Assess Their Preclinical Efficacy. *Toxins* **12**, 528 (2020).
65. Nerella, N. G., Block, L. H. & Noonan, P. K. The Impact of Lag Time on the Estimation of Pharmacokinetic Parameters. I. One-Compartment Open Model. *Pharm. Res.* **10**, 1031–1036 (1993).
66. Dockrell, H. M. & Smith, S. G. What have we learnt about BCG vaccination in the last 20 years? *Frontiers in Immunology* **8**, 1134 (2017).
67. Bashorun, A. O. et al. Intradermal administration of fractional doses of the inactivated poliovirus vaccine in a campaign: a pragmatic, open-label, non-inferiority trial in The Gambia. *Lancet Glob. Health* **10**, e257–e268 (2022).
68. Zhong, H., Chan, G., Hu, Y., Hu, H. & Ouyang, D. A Comprehensive Map of FDA-Approved Pharmaceutical Products. *Pharmaceutics* **10**, 1–19 (2018).
69. Baryakova, T. H., Pogostin, B. H., Langer, R. & McHugh, K. J. Overcoming barriers to patient adherence: the case for developing innovative drug delivery systems. *Nat. Rev. Drug Discov.* **22**, 387–409 (2023).
70. Ogunfowokan, O. Bite-to-hospital time and morbidity in victims of viper bite in a rural hospital in Nigeria. *Afr. J. Prim Health Care Fam Med.* **4**, 1–7 (2012).
71. Sharma, N., Chauhan, S., Faruqi, S., Bhat, P. & Varma, S. Snake envenomation in a north Indian hospital. *Emerg. Med. J.* **22**, 118–120 (2005).
72. Abouyannis, M. et al. A long-term observational study of paediatric snakebite in Kilifi County, south-east Kenya. *PLoS Negl. Trop. Dis.* **17**, e0010987 (2023).
73. Kazandjian, T. et al. Convergent evolution of defensive venom components in spitting cobras. *Science* **371**, 386–390 (2021).
74. Shoichet, B. K. Interpreting steep dose-response curves in early inhibitor discovery. *J. Med. Chem.* **49**, 7274–7277 (2006).
75. Mora-Obando, D., Fernández, J., Montecucco, C., Gutiérrez, J. M. & Lomonte, B. Synergism between basic Asp49 and Lys49 phospholipase A2 myotoxins of viperid snake venom in vitro and in vivo. *PLoS One* **9**, 1–11 (2014).
76. Pucca, M. B. et al. Unity makes strength: exploring intraspecies and interspecies toxin synergism between phospholipases A2 and cytotoxins. *Front. Pharmacol.* **11**, 1–10 (2020).
77. Bustillo, S. et al. Phospholipase A2 enhances the endothelial cell detachment effect of a snake venom metalloproteinase in the absence of catalysis. *Chem. Biol. Interact.* **240**, 30–36 (2015).
78. Takeda, S., Takeya, H. & Iwanaga, S. Snake venom metalloproteinases: structure, function and relevance to the mammalian ADAM/ADAMTS family proteins. *Biochim. Biophys. Acta.* **1824**, 164–176 (2012).
79. Beckett, R. P., Davidson, A. H., Drummond, A. H., Huxley, P. & Whittaker, M. Recent advances in matrix metalloproteinase inhibitor research. *Drug Discov. Today* **1**, 16–26 (1996).
80. Evans, J. D. et al. A phase II trial of marimastat in advanced pancreatic cancer. *Br. J. Cancer* **85**, 1865–1870 (2001).
81. Menzies, S. K. et al. In vitro and in vivo preclinical venom inhibition assays identify metalloproteinase inhibiting drugs as potential future treatments for snakebite envenoming by *Dispholidus typus*. *Toxicon X* **14**, 1–10 (2022).
82. Chowdhury, A. et al. Venom-induced blood disturbances by palearctic viperid snakes, and their relative neutralization by anti-venoms and enzyme-inhibitors. *Front. Immunol.* **12**, 1–14 (2021).
83. Warrell, D. A. & Arnett, C. The importance of bites by the saw scaled or carpet viper (*Echis carinatus*): epidemiological studies in Nigeria and a review of the world. *Acta Trop.* **33**, 307–341 (1976).
84. Amr, Z. S., Abu Baker, M. A. & Warrell, D. A. Terrestrial venomous snakes and snakebites in the Arab countries of the Middle East. *Toxicon* **177**, 1–15 (2020).
85. Warrell, D. A. et al. Poisoning by bites of the saw-scaled or carpet viper (*Echis carinatus*) in Nigeria. *Quart. J. Med.* **46**, 33–62 (1977).
86. Sasa, M. & Segura Cano, S. E. New insights into snakebite epidemiology in Costa Rica: a retrospective evaluation of medical records. *Toxicon X* **7**, 1–12 (2020).
87. Otero, R. et al. Complications of *Bothrops*, *Porthidium*, and *Bothriechis* snakebites in Colombia. A clinical and epidemiological study of 39 cases attended in a university hospital. *Toxicon* **40**, 1107–1114 (2002).
88. Cruz, N. S. & Alvarez, R. G. Rattlesnake bite complications in 19 children. *Pediatr. Emerg. Care* **10**, 30–33 (1994).
89. Maxmen, A. The fight to manufacture COVID vaccines in lower-income countries. *Nature* **597**, 455–457 (2021).
90. Pilkington, V., Keestra, S. M. & Hill, A. Global COVID-19 vaccine inequity: failures in the first year of distribution and potential solutions for the future. *Front. Public Health* **10**, 1–8 (2022).
91. Tilbury, C. R. Observations on the bite of the Mozambique spitting cobra (*Naja mossambica mossambica*). *S. Afr. Med. J.* **61**, 308–313 (1982).

92. Abouyannis, M. et al. TRUE-1: trial of repurposed Unithiol for snakebite envenoming phase 1 (safety, tolerability, pharmacokinetics and pharmacodynamics in healthy Kenyan adults). *Wellcome Open Res.* **7**, 1–33 (2022).
93. Issa, M. E. et al. Jadomycins are cytotoxic to ABCB1-, ABCC1-, and ABCG2-overexpressing MCF7 breast cancer cells. *Anticancer Drugs* **25**, 255–269 (2014).
94. Jaykaran. ‘Mean SEM’ or ‘mean (SD)’. *Indian J. Pharmacol.* **42**, 1–1 (2010).
95. Lazic, S. E., Clarke-Williams, C. J. & Munafò, M. R. What exactly is ‘N’ in cell culture and animal experiments? *PLoS Biol.* **16**, 1–14 (2018).
96. Hall, S. R. Histopathology images for Hall, et al., 2022. figshare <https://doi.org/10.6084/m9.figshare.19706761.v1> (2022).

## Acknowledgements

We would like to give our thanks to Paul Rowley for maintaining the snakes at the LSTM’s herpetarium and for routine venom extractions, Dr. Cassandra Modahl and Dr. Amy Marriott for their help with animal welfare observations during the in vivo experimentation, and Valerie Tilston and her team at the University of Liverpool for preparing the histopathology slides. The Authors acknowledge use of the Biomedical Services Unit provided by Liverpool Shared Research Facilities, Faculty of Health and Life Sciences, University of Liverpool. Funding was provided by a (i) Newton International Fellowship (NIF\R1\192161) from the Royal Society to S.R.H., (ii) a Sir Henry Dale Fellowship (200517/Z/16/Z) jointly funded by the Wellcome Trust and the Royal Society to N.R.C., (iii) a Wellcome Trust funded project grant (221712/Z/20/Z) to N.R.C. and J.K., (iv) a UK Medical Research Council research grant (MR/S00016X/1) to N.R.C. and (v) a UK Medical Research Council funded Confidence in Concept Award (MC\_PC\_15040) to N.R.C. This research was funded in part by the Wellcome Trust. For the purpose of open access, the authors have applied a CC BY public copyright licence to any Author Accepted Manuscript version arising from this submission.

## Author contributions

Conceptualisation: S.R.H., L.O.A., J.K., J.M.G., N.R.C. Methodology: S.R.H., S.A.R., J.M.G., E.C., C.A.D., N.R.C. Investigation: S.R.H., S.A.R., J.M.G., E.C., C.A.D., K.E.B., L.O.A., A.P.W., N.R.C. Data curation: S.R.H. Formal analysis: S.R.H., S.A.R., J.M.G., N.R.C. Original draft preparation: S.R.H., N.R.C. Editing: All authors.

## Competing interests

The authors declare no competing interests.

## Additional information

**Supplementary information** The online version contains supplementary material available at <https://doi.org/10.1038/s41467-023-43510-w>.

**Correspondence** and requests for materials should be addressed to Nicholas R. Casewell.

**Peer review information** : *Nature Communications* thanks Stephen Mackessy, and the other, anonymous, reviewer(s) for their contribution to the peer review of this work.

**Reprints and permissions information** is available at <http://www.nature.com/reprints>

**Publisher’s note** Springer Nature remains neutral with regard to jurisdictional claims in published maps and institutional affiliations.

**Open Access** This article is licensed under a Creative Commons Attribution 4.0 International License, which permits use, sharing, adaptation, distribution and reproduction in any medium or format, as long as you give appropriate credit to the original author(s) and the source, provide a link to the Creative Commons license, and indicate if changes were made. The images or other third party material in this article are included in the article’s Creative Commons license, unless indicated otherwise in a credit line to the material. If material is not included in the article’s Creative Commons license and your intended use is not permitted by statutory regulation or exceeds the permitted use, you will need to obtain permission directly from the copyright holder. To view a copy of this license, visit <http://creativecommons.org/licenses/by/4.0/>.

© The Author(s) 2023